Turbulence Modeling and Simulation in Hydraulics: A Historical Review

Wolfgang Rodi, M.ASCE[1]

Abstract: The paper reviews in condensed form and from a historical perspective the various methods for treating and simulating turbulence and its effects in hydraulic flows. After highlighting the main characteristic features of turbulence and the role it plays in hydraulics, a necessarily brief overview is given of the main methods used in hydraulic flow calculations for dealing with turbulence and its effects. These are (1) empirical relations, (2) methods solving the Reynolds-averaged Navier-Stokes (RANS) equations with the aid of statistical turbulence models, (3) direct numerical simulations (DNS), and (4) large-eddy simulations (LES). Brief comments are made on the historical development of the different methods, and for RANS, DNS, and LES methods some application examples are presented. For details on the individual methods and further application examples, the reader is directed to the very extensive literature. **DOI: 10.1061/(ASCE)HY.1943-7900.0001288.**

Author keywords: Turbulent flows; Hydraulic-flow calculations; Modeling; Empirical relations; RANS models; Direct numerical simulation; Large-eddy simulation.

Introduction

As in other fields of fluid mechanics, in hydraulics almost all flows, whether geophysical or man-made, are turbulent, i.e., they consist of a highly irregular, fluctuating, always three-dimensional eddying motion. Generally, the Reynolds numbers are large and so are disturbances introduced by irregular boundaries so that the laminar state with regular smooth motion is seldom found, except in groundwater flow.

The turbulent fluctuations contribute significantly to the transport of momentum, heat, and mass in hydraulic flows so that turbulence has a determining influence on the velocity, temperature, and concentration distribution in water bodies and hence on the flow development, the forces acting, the losses, heat transfer, the dilution of pollutants, sediment transport, and so on. Turbulence therefore plays an important role in most hydraulic problems, as will be shown by typical examples below.

The existence and importance of turbulence has been realized a long time ago and was hence studied by scientists and engineers. Already Leonardo Da Vinci observed the whirls that are so typical for turbulent flows [see his sketch reproduced on the cover of the book of Tennekes and Lumley (1972)]. In the second half of the nineteenth century, systematic studies of turbulence were started and also the first attempts to formulate descriptions of the phenomenon. Osborne Reynolds derived from experiments a dimensionless group for the onset and importance of turbulence (in pipe flow)—the Reynolds number. He also laid the foundations of the statistical treatment of turbulence by deriving averaged equations (1895). A few years earlier, Boussinesq (1877) had already proposed the treatment of turbulence by using an artificially increased viscosity (turbulent or eddy viscosity) in the governing equations. In the first decades of the twentieth century, it was primarily G. I. Taylor, L. Prandtl, and Th. Von Karman who advanced the knowledge on turbulence and proposed simple models for accounting for its effects. A historical review of these early studies can be found in the book of Levi (1995) and reviews of the work of these pioneers (but also later ones) in the book *A voyage through turbulence* by Davidson et al. (2011).

Because of the great importance of turbulence, there was not only a drive for understanding it but an increasing need for the ability to predict its effects. An essential part in most calculations of hydraulic flows is therefore the treatment of turbulence effects. In practice, until the advent of the computer in the 1960s, these effects were treated rather crudely and globally by empirical formulas, mostly in the context of one-dimensional (1D) analytical approaches. Such global methods are well covered in the books of Rouse (1946). Empirical relations are certainly very useful in practice, but only for solving simple problems and not for situations with complex boundary conditions and interactions of various flow regimes and different flow phenomena. Advances in computer technology opened up the possibility of tackling such problems by solving numerically the multidimensional differential equations governing them, with realistic boundary conditions. However, initially, until the 1980s, with exceptions only mean-flow equations could be solved in which the turbulent fluctuations are averaged out—the Reynolds-averaged Navier-Stokes (RANS) equations. In these, turbulence has to be accounted for by a statistical turbulence model—a RANS model—which determines the effect of turbulence on average (or mean) quantities, not resolving the actual turbulent motion.

Then, starting already in the 1970s, but primarily in the 1980s, computers became sufficiently powerful that the original time-dependent Navier-Stokes equations could be solved in a direct numerical simulation (DNS), resolving motions of all scales and hence not requiring a model, at least for very simple configurations and low Reynolds numbers. At the same time, for more realistic situations, large-eddy simulations (LES) were introduced and started to be applied. In LES, the turbulent motion is resolved only to the scale of the numerical grid and the fluctuating motion of the scale smaller than the mesh size is modeled by a subgrid-scale model. In recent years, with the availability of very powerful, high-performance computers, these methods saw a thriving

[1]Emeritus Professor, Karlsruhe Institute of Technology, Kaiserstr. 12, 76131 Karlsruhe, Germany. E-mail: rodi@kit.edu

Note. This manuscript was submitted on May 6, 2016; approved on October 11, 2016; published online on February 21, 2017. Discussion period open until July 21, 2017; separate discussions must be submitted for individual papers. This paper is part of the ***Journal of Hydraulic Engineering***, © ASCE, ISSN 0733-9429.

development, with LES, in particular in combination with RANS in a hybrid model, reaching the state of becoming a tool for practical calculations.

In this paper, the different types of methods for treating and simulating turbulence and its effects in hydraulic flows are reviewed from the perspective of their historical evolution. In a journal paper, such a review cannot be detailed; hence frequent reference is made to publications which, at their time, provided state–of-the-art reviews on various topics. Also, the paper can only cover the mainstream of turbulence calculation methods and not all methods that have been proposed and are in use. Further, with respect to previous publications, only a small sample can be included, with admittedly some bias toward the work of the author, which is difficult to avoid. Before the evolution of the different methods is discussed, a brief introduction is given to the main features of turbulence and to the role turbulence plays in hydraulics.

Main Characteristic Features of Turbulence

General introductions to the subject of turbulence are given in a variety of books, among them works by Bradshaw (1971), Tennekes and Lumley (1972), Pope (2000), and Davidson (2004); the first one is recommended for a quick and easy entry. An excellent introduction explaining and visualizing the most important features of turbulence can be found in the old but by no means outdated film of Stewart (1969). Focusing on hydraulics, the subject of turbulence in open-channel flow is covered comprehensively in the book of Nezu and Nakagawa (1993).

Turbulence is a very complex phenomenon as the turbulent motions are highly irregular, fluctuating and always three-dimensional (3D). The turbulent fluctuations cause strong mixing of all flow quantities and hence momentum, heat, and mass transfer that is usually much larger than the transfer resulting from Brownian motion in a laminar flow, which in contrast to turbulence is smooth and regular. The differences between laminar and turbulent flow are illustrated in Fig. 1 by a dye-visualization picture of a 3D wall jet, depicting the lateral spreading. The flow issuing from a square outlet is first laminar, showing smooth motion with little mixing with the ambient fluid and hence hardly any spreading. Then the shear layers at the edges of the laminar jet become unstable and the flow breaks up abruptly into highly irregular turbulent motion with strong fluctuations that entrain ambient fluid and cause the jet to spread significantly. This is also the typical behavior found in free jets. The strong mixing caused by the

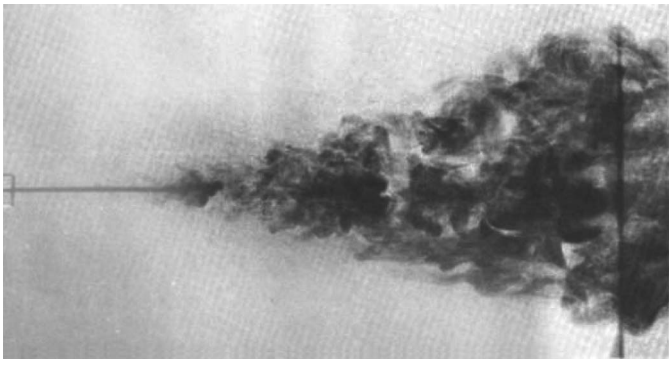

Fig. 1. Dye-visualization picture of 3D wall jet issuing from a square outlet at R = 1,100; view normal to the wall (reprinted from Launder and Rodi 1983)

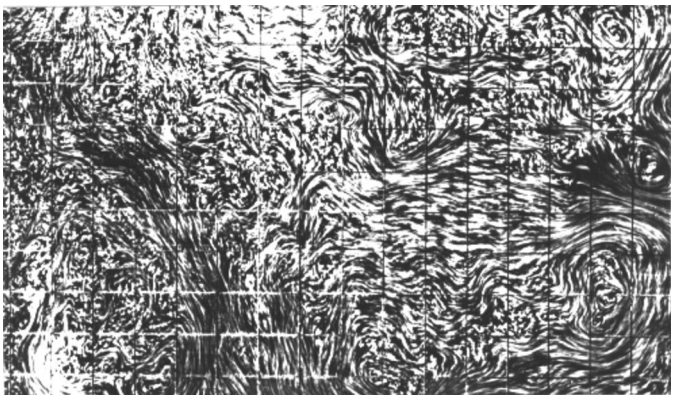

Fig. 2. Turbulent eddies at the surface of a stirred tank (courtesy of Reinhard Friedrich)

turbulent fluctuations is the practically most important feature of turbulence.

The turbulent motion consists of eddies that carry rotation and represent a tangle of vortices stretching each other, thereby generating smaller eddies and passing on kinetic energy to them until the fluctuations are damped by viscous forces at the smallest eddies. Because of this process, called energy cascade, the turbulent motion usually consists of a wide spectrum of eddy sizes, as is visualized in Fig. 2 by the motion at the surface of a stirred water tank. An example of a spectrum is given in Fig. 3, exhibiting the distribution of the kinetic energy of the turbulent fluctuations with wave number k, which is inversely proportional to the eddy size. The largest eddies (small k) are of the extent of the flow domain; they contain most of the energy of the fluctuations. They are also most effective in the transfer process and hence the mixing. The smallest eddies with high fluctuation frequencies are controlled by viscosity and here dissipation takes place. The width of the spectrum increases with Reynolds number, as shown in Fig. 3; i.e., the dissipation range shifts to higher wave numbers and hence smaller eddies. This has important consequences for

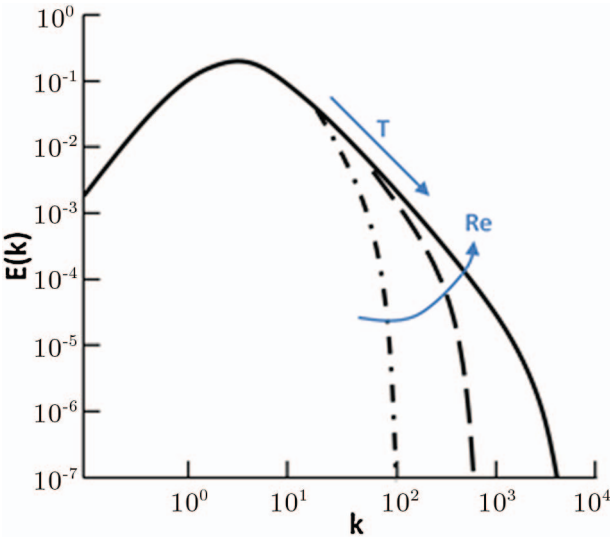

Fig. 3. (Color) Spectra of isotropic turbulence with increasing Reynolds number (adapted from Fröhlich 2006)

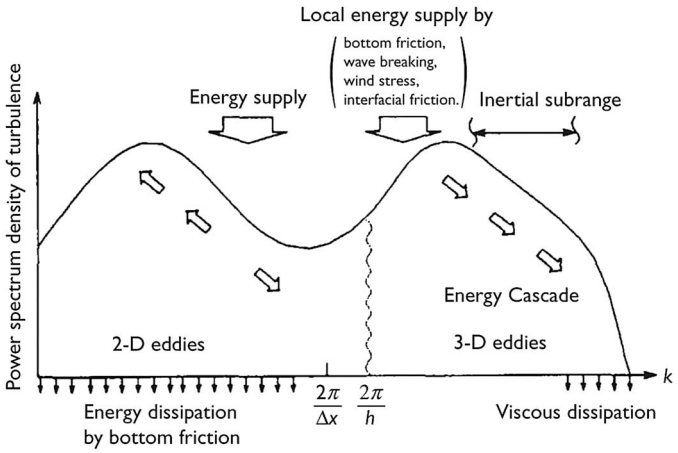

Fig. 4. Two-range energy spectrum in shallow-water flow (reprinted from Nadaoka and Yagi 1998, © ASCE)

eddy-resolving calculation methods such as DNS and LES (see later sections on these methods).

A different kind of spectrum, namely a two-range spectrum, can exist in shallow water flows, as shown schematically in Fig. 4. Here, because the horizontal extent of the water body is much larger than the vertical one, predominantly two-dimensional horizontal eddies can exist with sizes considerably larger than those of the bed-friction–generated 3D turbulence that is restricted by the water depth. The low wave-number range in Fig. 4 is the spectrum of the two-dimensional (2D) horizontal eddies, and the high wave-number range represents the spectrum of the 3D eddies with size smaller than the water depth. The large 2D eddies are responsible for the horizontal mixing in shallow flows and the 3D bed-generated eddies for the vertical mixing.

The small-scale, dissipative motions are fairly random, while the large-scale fluctuating motions, which interact with the mean flow and depend on the boundary conditions, often have some order and some correlated behavior representing coherent structures. These structures have a lifecycle of birth, convection by the mean motion, mutual interaction, and finally breakdown. Eddy-resolving techniques such as DNS and LES simulate this cycle and hence the behavior of the structures. In methods based on statistical averaging, coherent structures are not dealt with explicitly. Only their effect on the mean flow is accounted for through a RANS model. Examples of coherent structures are shown later in the sections on DNS and LES.

Role of Turbulence in Hydraulics

Turbulence in natural rivers is usually quite strong because of the irregular boundaries and the large roughness of river beds, particularly so for flood situations with vegetated beds. Turbulence is generated by high shear near the bed and in free-shear layers it is formed by flow separation past roughness or vegetation elements or artificial structures such as piers, groynes, abutments, and so on. The turbulence has a determining influence on the flow field and on the friction and pressure forces acting on the bounding solid surfaces and consequently on the discharge and the water level. In channels of noncircular cross section, turbulence-driven secondary motions develop that may suppress the velocity maximum below the surface. Turbulence keeps sediment particles in suspension, causes the erosion of particles from the bed, and controls the gas exchange at the water surface. Further, turbulence causes mixing and thereby dilution of pollutants. It is responsible for the mass exchange with embayments and hence for the washing out of pollutants from these.

In man-made conduits such as canals and water and wastewater networks, and in hydraulic machinery, turbulence is no less important and has the main effect of causing losses. Such losses are particularly strong when flow separation occurs so that high turbulence is generated.

Coastal waters, lakes, and reservoirs have generally wider extensions in all directions than the flows covered above and are therefore subjected to different turbulence-generation mechanisms. During certain times, solar radiation heats the surface layers, setting up a stable stratification and in particular a thermocline separating the warmer surface water from the colder water below. Wind shear generates turbulence in the surface layer, leading to strong mixing there and a fairly uniform temperature distribution. Similarly, cooling the surface at night and in winter sets up an unstable stratification, also generating turbulence in a process called penetrative convection. Turbulence from both origins erodes the stable stratification and the thermocline, entraining colder water from below, thereby deepening the warmer surface layer.

In the water bodies just discussed, there may be inflows, e.g., from rivers or artificial discharges. When these inflows are along the bed and have a density different from the receiving water body, density currents develop. The spreading of such currents is strongly influenced by turbulence. Discharges of waste by single or multiple jets in all kinds of water bodies are also largely determined in their behavior by turbulence, which causes the spreading and mixing discussed earlier and hence the dilution of the waste and the distribution of contaminants.

As a final example of hydraulic flows with turbulence effects, sedimentation tanks are mentioned as they are used in various forms of clarifiers and wastewater treatment plants as well as intakes of hydropower plants. In these tanks, solid waste particles need to be separated from the water by the settling process. This process is counteracted by turbulence and depends strongly on the flow developing in the tank. This itself is controlled to a large extent by the turbulence generated in the discharge jets and the flow around deflectors used to prevent short circuiting, but on the other hand it is damped by the stable stratification set up by the density differences as a result of the particle-laden discharge. Turbulence also has a determining influence on the flocculation of particles, which on the other hand determines their settling. Hence, altogether, turbulence plays an important role in sedimentation tanks and has a major effect on their efficiency.

Empirical Relations

Until the advent of the computer in the 1960s, the effects of turbulence in hydraulic flow problems could be treated only in a highly empirical way. With the aid of dimensional analysis, experimental information was condensed into many useful formulas, which could be employed directly for determining the flow behavior of interest. Probably the first one was the friction law introduced by Chezy in 1770, which corresponds closely to the Darcy-Weissbach formula introduced in the middle of the nineteenth century. This relates the friction in a closed conduit to the hydraulic radius and the square of the velocity, introducing a dimensionless friction coefficient that depends on the Reynolds number and the wall roughness. This dependence is given in a general way by a diagram devised by Moody (1944), which became very popular. The Darcy-Weissbach relation can be transformed into a flow formula for open-channel flow, but in practice, in particular for natural rivers, the somewhat different empirical

Gauckler-Manning-Strickler (GMS) formula is mostly used. This formula was introduced first by Gauckler (1868), then independently by Manning (1889), and later substantiated by Strickler (1923). The dimensional Manning coefficient n (inverse of the Strickler coefficient k_{st}) appearing in this formula depends strongly on the roughness and geometry of the channel. Values can be found in handbooks and books on open-channel flow (e.g., Chow 1959; Henderson 1966; Chaudhry 2008).

Empirical formulas are also in use for calculating local losses as a result of flow separation and the associated turbulence occurring when the flow geometry changes abruptly, in bends and past immersed structures (e.g., piers, abutments). Such formulas are also used for determining the drag of immersed bodies. Further, from the middle of the twentieth century onward, formulas were proposed for the global sediment transport of suspended and bed load (e.g., Meyer-Peter and Müller 1948; van Rijn 1993). For simple jets and plumes (no cross flow, no ambient stratification, no interaction with boundaries), empirical formulas developed with the aid of dimensional analysis and scaling laws allowed the prediction of the spreading and decay of velocity and pollutant concentration and hence the dilution of discharged substances (Chen and Rodi 1980; List 1986). Empirical formulas exist also for estimating the plume rise in a stably stratified environment.

Turbulence is treated by empirical relations also in calculation methods based on reduced forms of conservation laws for mass, momentum, energy, and species concentration. Such methods, in some application areas called integral methods, perform a 1D analysis for flows with layer characteristics that have a predominant flow direction such as in conduits, rivers, jets, plumes, and horizontal layers in lakes and reservoirs. The 1D equations, obtained by integrating the originally 3D governing equations over the flow cross section (layer) with the aid of profile assumptions (often uniform) are solved to obtain the development in flow direction of flow quantities characteristic for the cross section (e.g., average velocity, concentration, layer width). Turbulence controls the flux of conserved quantities across the boundaries of the cross section (layer), such as entrainment (mass flux) into jets and plumes; friction (momentum flux) in conduits or layer interfaces in lakes; and heat or mass (e.g., sediment) flux at the bed or surface of rivers. These fluxes are estimated through empirical relations, such as the friction laws mentioned previously; entrainment laws for jets and plumes; and relations for heat and mass exchange at surfaces, whether they are free surfaces or walls.

For simple flow configurations, the 1D integral equations can be solved analytically. For more complex situations, as they usually occur in practice, computer models need to be employed, such as models for networks of natural or constructed channels. An example is the widely used program *HEC RAS* (developed by the U.S. Army Corps of Engineers, Davis, California), which employs the GMS relation for determining the losses. Another program of this type is *DYRESM* of Imberger and Patterson (1981) for predicting the vertical temperature and salinity distribution in lakes and reservoirs. In this, 1D integral equations are solved for individual horizontal layers with mixing across the layers and surface fluxes accounted for through empirical relations. Integral models are also used in discharge models for calculating the mixing in outfalls. An example is the *CORMIX* system (Doneker and Jirka 1991, 2001), in which the integral method is combined with other semiempirical methods to account for the interaction of outfall jets and plumes with boundaries, thereby yielding a fairly general calculation procedure used in practice.

The mixing of substances in water bodies is another area where empirical relations have been much used. This subject is treated comprehensively in the book of Fischer et al. (1979). Considering the case of a river, the distribution of substances, whether discharged into the river or resulting from the merger of different streams, is governed by the originally 3D convection-diffusion equation in which, for the methods considered here, the turbulent mixing is accounted for by a turbulent diffusivity (called mixing coefficient) obtained empirically. RANS models discussed in the next section also mostly employ a turbulent diffusivity but determine this with the aid of a turbulence model. In open channels the mixing coefficient is taken to be proportional to the local flow depth h and the friction velocity u^*, the proportionality factor Γ depending on the direction of mixing. As vertical mixing is fairly rapid, of main interest is the depth-averaged transverse mixing (factor Γ_y). Fischer et al. (1979) report that in straight laboratory flumes values in the range $\Gamma_y = 0.1-0.2$ have been measured by dye-spreading experiments. However, transverse spreading of dye is not only a result of turbulence but also of dispersion caused by nonuniform vertical concentration distribution and the secondary motions present. These can have a strong effect. Large-eddy simulations (Hinterberger et al. 2008), in which these dispersion effects could be excluded, yield a value at the lower limit $\Gamma_y = 0.1$. In natural rivers with bends and irregular geometry, the secondary motions are usually fairly strong, so that the dispersion effects dominate and consequently much higher transverse mixing coefficients have been measured. Fischer et al. (1979) gave a value of $\Gamma_y = 0.6 \pm 50\%$. Further, longitudinal turbulent mixing is also unimportant in rivers because the shear-flow dispersion is much larger and can be accounted for by a longitudinal mixing coefficient.

The friction velocity u^* itself is usually related empirically to the local depth-average velocity by a quadratic friction law introducing a friction coefficient c_f. This is closely related to the friction laws discussed earlier and can be directly calculated from these, e.g., for rough beds from the Manning coefficient n. The bed friction thus determined is also used extensively in calculating the depth-averaged flow by solving the 2D shallow water equations, thereby accounting for the vertical turbulent mixing of momentum in the flows. Often the horizontal turbulent mixing of momentum, in contrast to the mixing of scalars, is of subordinate importance compared to other terms in the equations and can be neglected; if it is of relevance, it can be accounted for through a RANS turbulence model or through 2D LES, as discussed in later sections on these methods.

RANS Turbulence Models

Empirical formulas and integral models that only treat turbulence globally are only suitable for relatively simple situations and not for complex geometries. When there are more than just a few parameters determining the flow and complex interactions between various flow phenomena take place, such methods are not applicable. Also, the methods do not yield details of the flow development and the distribution of prime quantities of interest. For providing these and for general applicability, field methods are necessary that employ the governing equations in their original form and account locally for turbulence effects.

The equations governing the flow, including all details of the complex turbulent motion, are known—namely the time-dependent Navier-Stokes equations—and today they can be solved numerically for certain flows, as described in the next section. However, this was not possible until powerful computers became available a few decades ago. So, until then, there was no hope of being able to solve the original Navier-Stokes equations, and recourse had to be

taken to statistical methods. In these, turbulence is averaged out and equations are solved for mean-flow quantities, which are of prime interest in practice anyway.

The foundations of the statistical treatment were laid in 1895 by Osborne Reynolds. He decomposed the instantaneous velocity components u_i into mean velocity components $\bar{u}_i$ and fluctuations u_i' around the mean and formally time-averaged the Navier-Stokes equations. The resulting equations governing the mean velocity are called the Reynolds-averaged Navier-Stokes (RANS) equations. They are given in ASCE (1988) and Rodi (1980, 1993b). Because of the nonlinearity of the convection terms of the Navier-Stokes equations, the splitting-up and averaging process leads to the appearance of additional terms, which are correlations of fluctuating velocities $\overline{u_i'u_j'}$; these act as stresses on the fluid (in addition to the viscous stresses) and are called turbulent or Reynolds stresses. Because of their appearance, the equations are no longer closed and a turbulence model—a RANS model—is needed to determine the stresses. When the mean flow is unsteady, such as in tidal or vortex-shedding flows, the time-averaging is carried out only to remove the turbulent fluctuations and not the unsteadiness of the mean motion, and the model is used in an unsteady (URANS) mode.

Already 18 years earlier, without formally introducing the stresses, Boussinesq (1877) proposed to account for the effect of turbulence by replacing in the Navier-Stokes equations the molecular viscosity with a larger, artificially introduced viscosity—the turbulent or eddy viscosity. This is, however, not a fluid property but depends on the local state of turbulence; it is a priori unknown and hence its local value must be determined by a turbulence model, as described later in this section. The first model allowing this, and hence the first proper turbulence model, was proposed by Prandtl (1925) and is known as the mixing-length model. This model relates the eddy viscosity to mean velocity gradients and an empirically prescribed length scale of turbulence, the mixing length. Beginning in the 1940s, models were developed that are based on transport equations for turbulence quantities (such as Reynolds stresses, turbulence energy, length scale, and dissipation rate); (e.g., Prandtl 1945; Kolmogorov 1942; Rotta 1951). These were quite advanced, reaching the level of what is used today, but they could not be tested and applied because the equations could not be solved except for very simple flows. With the advent of computers in the 1960s and the development of numerical methods for solving the equations, the situation changed and the models, starting with the simpler ones, could be tested for a variety of flows. This activity took place primarily in the area of mechanical and aerospace engineering, and landmark events included the 1968 Stanford Conference on Boundary Layers (Kline et al. 1969) and the 1972 NASA Langley Conference om Free Shear Flows (NASA 1972), where for set test cases calculations obtained with various models were compared. The 1970s and early 1980s saw the development of further, more advanced, and in principle more generally applicable models, and in 1980 and 1981 the performance of these was compared for a fairly wide range of flows at conferences held at Stanford University (Kline et al. 1981), called the Stanford Olympics. Soon after, the research activity in this field slowed and shifted to large-eddy simulations (LES) and later also to the use of RANS models in hybrid RANS/LES methods. Comprehensive information on RANS turbulence models, not geared to hydraulics, can be obtained from a number of fairly recently published books (Wilcox 2006, 1993; Durbin and Pettersson-Reif 2001; Launder and Sandham 2004; Hanjalic and Launder 2012; Leschziner 2016).

In hydraulics, refined turbulence models started to be used a little later than in mechanical and aerospace engineering, namely in the mid-1970s. The most important and commonly used models are reviewed and discussed briefly below. Detailed reviews and a full description of turbulence models in hydraulics can be found in a number of publications. Rodi (1980, 1993b) presented the first review, summarizing the knowledge and experience gained by the end of the 1970s. Later, Rodi (1987) reviewed RANS models for stratified flows and covered models for use in coastal, estuarian, and harbor situations (1993a). By the mid-1990s, considerable experience had already been gained with RANS models in hydraulics and Rodi (1995) reviewed their effects on the field. Somewhat earlier, the ASCE Task Committee on Turbulence Models in Hydraulics (ASCE 1988) presented and evaluated RANS models available in the mid-1980s. Burchard (2002) gave a review of RANS modeling for marine waters. Lyn (2008) provided a detailed treatise on the subject of turbulence modeling of relevance for sediment transport calculations. Some of these overview publications are somewhat dated, but apart from a few more recent developments mentioned below, they cover largely the models in use to date in hydraulics. They provide all the relevant equations, so that these are not repeated here, and they also present a wide variety of application examples. Over the decades, many additional applications have been published in the literature. These cannot all be reviewed and cited here, but some examples will be presented below of recent applications to situations close to reality in practice.

RANS Models in Use in Hydraulics

Most calculations in hydraulics have been and still are carried out with linear eddy viscosity/diffusivity models (employing a linear relation between turbulent stresses and velocity gradients). More refined models exist but are seldom used in hydraulics and will hence be touched upon only briefly.

The simplest approach is to use a constant eddy viscosity/diffusivity whose value is prescribed empirically (methods of previous section) or determined by trial and error calculations. This approach is suitable only for large-water body calculations and is still commonly used for these [e.g., in the code *Telemac* (Hervouet and Bates 2000)], but it is too crude for near-field calculations around structures and discharges and for resolving the vertical structure of the flow. In any case, when used in large-water-body calculations the approach is of little relevance for solving the momentum equations as these are dominated by other terms. On the other hand, the diffusivity chosen in the convection-diffusion equation has a determining influence on the distribution of scalars. Empirical relations for determining this diffusivity have already been discussed in the previous section.

For determining local values of the eddy viscosity ν_t and diffusivity Γ_t, it is important to note that, for dimensional reasons, these quantities are proportional to a velocity scale V and a length scale L characterizing the (large-scale) turbulent motion. Further, invoking the Reynolds analogy, the eddy diffusivity is usually assumed to be proportional to the eddy viscosity, i.e., $\Gamma_t = \nu_t/\sigma_t$, with the turbulent Prandtl/Schmidt number σ_t taken as (empirical) constant.

The first model for describing the distribution of the eddy viscosity over the flow field is the mixing-length model proposed by Prandtl (1925). It relates the turbulent velocity scale V to the local mean velocity gradients and an empirically prescribed mixing length l_m. The model is simple and robust, but the empirical input specification of l_m is problem dependent, and the model implies the assumption of local equilibrium of turbulence production and dissipation so that it cannot account for transport and history effects of turbulence. Also, prescribing l_m for situations with complex geometry is difficult. Because of its simplicity, the model is still used in practical flow calculations by commercial codes for simulating the

vertical turbulent transport as well as in a Smagorinsky version (relating l_m to the numerical mesh size—see section on LES) for the horizontal transport.

In order to account for transport and history effects of turbulence, so-called one-equation models were developed that solve one transport equation for a characteristic turbulence quantity. This can be either the turbulent kinetic energy k (yielding the velocity scale $V = k^{1/2}$ and requiring again an empirical length-scale prescription) or the eddy viscosity ν_t itself. The Spalart and Allmaras (1994) model is of the latter type and is popular in aerospace applications, but not in hydraulics. A model of the former type is available as an option in commercial and open-source codes (e.g., *DELFT3D*), but it is probably not used widely.

Two-Equation Models

The simplest models that do not require an empirical prescription of the length scale or of any other turbulence quantity inside the calculation domain are two-equation models. These solve in addition to the k-equation for the velocity scale a second transport equation for determining the length scale L. This equation may not necessarily have L itself as a dependent variable but can have any combination of the form $Z = k^m L^n$. Various combinations have been proposed and tested (Rodi 1993b; Leschziner 2016), but early in the 1970s the equation for the dissipation rate $\varepsilon = k^{3/2}/L$ emerged as the most popular. The k-ε model based on it dominated the field of RANS calculations for many years. The model was very widely tested and applied in all fields of engineering, including hydraulics, and also for geophysical flows, and it has been implemented in virtually all commercial CFD codes, including those used in hydraulics. The standard model described first by Launder and Spalding (1974) uses wall functions to bridge the viscosity-affected regions near walls. A number of low-Reynolds-number versions (Patel et al. 1985) have been developed that allow integration of the equations to the wall, but these are more cumbersome and expensive to use so that in hydraulics mostly the standard version is employed. A different version of the model was derived by Yakot and Orszag (1986) based on renormalization group theory. This version has an additional term in the ε-equation. The RNG version, which is also used in hydraulics, was found to perform better than the standard version in some flows, but worse in others—see a discussion by Lyn (2008). Special versions of the k-ε model were developed for free-surface flows and for flows with buoyancy effects, as described by Rodi (1993b, 1987).

In the many tests and applications, the k-ε model was found to be applicable to a wide variety of flows with reasonable success, but in certain situations the model does not produce satisfactory results. Problematic flows are those with an adverse pressure gradient and when anisotropy of turbulence and special effects like streamline curvature play an important role. A useful brief summary of the weaknesses of the k-ε model is given in the *Best practice guidelines* of Casey and Wintergerste (2000). A disadvantage of the low-Reynolds-number versions for integration to the wall is that they involve special near-wall damping functions that hamper the numerical solution. This and the weakness in adverse pressure-gradient boundary layers, causing late prediction of separation, promoted in recent years the increased use of the k-ω model, which instead of the ε-equation uses an equation for the turbulence frequency $\omega = k^{1/2}/L$ to determine the length scale L. This model, originally proposed by Wilcox (1993) does not require damping functions near walls and performs better in adverse-pressure-gradient flows, but suffers from excessive sensitivity to the boundary condition for ω at free-stream boundaries. This prompted Menter (1994) to blend the two models so that the k-ω model is active near walls and the k-ε model is active away from walls. In addition, he introduced a shear-stress limiter that in flows with high strains makes the shear stress proportional to the kinetic energy k, a measure beneficial in adverse-pressure-gradient flows. The resulting model, called the Menter SST model, has become more and more preferred to the k-ε model, especially in the fields of mechanical/aerospace engineering, but it is also used in hydraulics.

In geophysical flows, the k-kL model of Mellor and Yamada (1982) has found fairly wide application. This determines L from an equation for kL. Mellor and Yamada, as well as other turbulence modelers, criticized the use of the ε-equation because the process of dissipation is associated with the small-scale turbulence, while the length scale L to be determined should be characteristic for the large-scale motion. The amount of energy dissipated (dissipation rate ε) is controlled, however, by the energy transferred from the large-scale to the small-scale motion, and hence ε is a parameter characterizing the large-scale motion. Therefore, the criticism is not well founded and, after all, the ε- and kL-equations, both being fairly empirical, perform in a similar way. One difference is that the kL-equation requires an additional near-wall term, while the ε-equation does not.

Second Moment Closures and Algebraic Models Derived from Them

A comprehensive and recent account of models not based on the eddy viscosity/diffusivity concept but solving model transport equations for the individual turbulent stress and flux components can be found in the book of Hanjalic and Launder (2011). Models of this type are in principle superior to eddy viscosity/diffusivity models as they represent better the physical processes. They allow the prediction of turbulence-driven secondary motions in channels and of free-surface and stratification effects in a natural way. However, they are considerably more demanding in terms of boundary conditions and the numerical solution. Hence they are so far not used much in practice, not even in mechanical/aerospace engineering, and hardly in hydraulics.

In order to reduce the numerical solution effort, the stress/flux-equation models were simplified to algebraic stress/flux models by introducing model assumptions for the differential convective and diffusive transport terms (Rodi 1987, 1993b). These models account for anisotropy of turbulence and buoyancy effects and can predict the secondary motions in open-channel flow (Naot and Rodi 1982). The 2½-level model of Mellor and Yamada (1982) is of this type and is used in the area of marine waters. Most advanced is the explicit algebraic stress model of Wallin and Johansson (2000), and this has become the most popular in mechanical/aerospace engineering, but it is hardly used in hydraulics.

Models for Depth-Averaged Calculations

The models discussed so far are for applications in 3D flows or genuinely 2D flows. In shallow water situations, mostly 2D equations are solved. These equations are obtained by depth-averaging the original 3D equations, and they describe the distribution of depth-averaged horizontal velocity components, temperature, or concentration; they are given by ASCE (1988) and Rodi (1993b). The equations contain depth-averaged (DA) turbulent stresses and fluxes representing the horizontal turbulent momentum and scalar transport through vertical planes reaching from the bed to the surface. Vertical fluxes appear only on the boundaries as bed and surface shear stresses, heat and gas transfer at the surface, and sediment exchange with the bed. These boundary fluxes are treated by empirical relations as discussed already in the previous section.

In many situations, especially in far-field ones, the bed friction dominates in the momentum equations over the horizontal stresses,

which are therefore often neglected. However, in near-field situations around structures and outlets, these stresses are of relevance. On the other hand, in the scalar transport equations, the horizontal fluxes are always important. The depth-averaged equations also contain dispersive terms arising from nonuniformity of velocities and scalars over the depth, as discussed above. The physical effect of these cannot be distinguished from that of the turbulent fluxes, but they do not represent turbulence and basically require special modeling. In the momentum equations, these terms are usually again not important, but they can have a dominant influence on the scalar distribution, especially in the presence of secondary flows and in unsteady situations (Fischer et al. 1979).

All models in common use for DA horizontal turbulent stresses and fluxes are based on the eddy viscosity/diffusivity concept; they differ by how the DA viscosity $\tilde{\nu}_t$ and diffusivity $\tilde{\Gamma}_t$ ($=\tilde{\nu}_t/\sigma_t$) are determined. Again constant values are often used in large-water body calculations, where $\tilde{\nu}_t$ is usually of little relevance, but an appropriate value of $\tilde{\Gamma}_t$ has to be chosen empirically. This accounts usually also for the dispersion effects.

The turbulence causing the horizontal fluxes has a two-range spectrum as sketched in Fig. 4: it consists of smaller-scale bed-generated 3D turbulence and of larger-scale 2D eddies generated by horizontal velocity gradients. In general, both components need to be represented in a realistic model for $\tilde{\nu}_t$. The simplest way to account for bed-generated turbulence is through the Elder (1959) model, also labeled the parabolic model. This is based on the parabolic vertical distribution of ν_t in developed channel flow, which upon integration yields the DA value $\tilde{\nu}_t = \kappa/6u^*h$, which with the von Karman constant $\kappa = 0.41$ results in $\tilde{\nu}_t = 0.07u^*h$. This is sometimes used as the sole model for the DA horizontal transport. In other calculation methods, which account for the transport attributable to large-scale horizontal eddies by resolving these (called either DA-URANS or 2D LES; see the section on LES), the Elder model only features as a sub-depth-scale model. As $\sigma_t = 0.5-0.7$, the Elder model yields a DA eddy diffusivity $\tilde{\Gamma}_t$ of 0.1–0.14, as discussed already in the section on empirical relations. To account for transport of turbulence generated by horizontal velocity gradients, the Elder model was also extended by simply adding to $\tilde{\nu}_t$ a component determined by a mixing-length model (Wu et al. 2004; Lea et al. 2007).

Rastogi and Rodi (1978) developed a DA version of the k-ε model that accounts for both bed-generated sub-depth-scale turbulence and larger-scale turbulence generated by horizontal velocity gradients. In the absence of such gradients, the model reduces to the Elder model. The DA eddy viscosity is related to DA values of k and ε, which are obtained from transport equations for these quantities. The equations contain two production terms, one attributable to horizontal velocity gradients and the other to bed-generated turbulence; the latter is therefore related to u^*. The DA version of the k-ε model introduces one additional empirical constant, namely the dimensionless diffusivity $\Gamma^* = \tilde{\Gamma}_t/hu^*$ derived from dye-spreading experiments. For developed channel flow, the value $\Gamma^* \approx 1.3$ is appropriate (see previous section), but by increasing the value the often considerable effects of dispersion can be accounted for. The model has been widely used and tested (e.g., Rodi et al. 1981; Rodi 1984) and has also been implemented in commercial codes. Various modifications have been suggested (e.g., Booij 1989; Wu et al. 2004; Lea et al. 2007).

URANS Approach

RANS models are used increasingly also in unsteady (URANS) mode, not only per se but also in hybrid LES/RANS calculations. Thereby the time-dependent forms of the statistical equations are solved. In this case the statistical quantities are averages over a time considerably larger than the timescale of the turbulent motion but small compared with the timescale of the unsteady mean motion. Classical cases where this scale separation prevails are flows with unsteady boundary conditions such as tidal and wave-induced flows, variable discharges, and flows with changing bed morphology, but also situations with steady boundary conditions that are inherently unsteady because of an internal instability as in the case of vortex shedding, whose motion is not considered as turbulence. Hence, within the RANS concept, what is (or is considered as) turbulence is modeled. There are, however, gray areas: it is clear that in genuinely 2D calculations, URANS does not resolve turbulence, as this is by its nature a 3D motion; the situation is different for 3D URANS, where formally the same averaged Navier-Stokes equations are solved as in LES (see the section on LES). Only the way the effective (eddy) viscosity is determined is different. When a RANS model producing low enough eddy viscosity is used, 3D URANS calculations can resolve part of the turbulent motion [e.g., the SAS method of Menter and Egorov (2010)]. This and the relation to LES are discussed in some detail by Palkin et al. (2016). However, most RANS models yield a high level of eddy viscosity and hence enough damping so that turbulent motions are usually not resolved in 3D URANS calculations and need to be fully accounted for by the model. As discussed in the section on depth-averaged (DA) LES, DA URANS is also formally identical to DA LES, and here even the same sub-depth-scale model is used to account for the unresolved 3D turbulent motion.

Application Examples

Over the last four decades, many hydraulic flow calculations with RANS models have been carried out and published, starting with more fundamental ones but increasingly to solve engineering problems of a wide variety. Here only a few application examples can be presented, selected to represent different application areas and situations close to reality in practice.

The first example concerns 2D calculations with the DA k-ε model of flow in the Rhine River during a flood event in 1993. A 10-km stretch near Vynen-Rees was simulated by Minh Duc (1998) over a time of 31 days, with topography, discharge distribution, and water level at control points provided as input. Different roughness coefficients were used for riverbed and floodplains and were adjusted to yield water levels corresponding to field measurements. The model was validated first for a substretch under steady, unflooded conditions by comparing velocity profiles with laboratory measurements carried out at the Bundesanstalt für Wasserbau - German Federal Waterways and Engineering Institute (BAW). Fig. 5 shows the topography and the DA velocity as well as the flooded areas during rising, peak, and falling flood. The results were found to be in good qualitative agreement with observations recorded during the real flood event.

The examples to follow are all 3D calculations. The BAW was charged with investigating an accident of the barge TMS *Waldhof*, which capsized and ran aground in a stretch of the Rhine near Loreley. The BAW conducted 3D simulations of the flow in the relevant stretch with a commercial code using the k-ω turbulence model and 5 million grid points [for a brief description, see (Wenka et al. 2016)]. The forces on and the movement of the barge were also simulated until it capsized. For the region around the barge, Fig. 6 shows contours of the predicted vertical velocity, which has a major effect on the stability of the barge and is hence of relevance for investigating the accident.

The next example concerns flow and sediment transport in a stretch of the Elbe River that includes the former border of

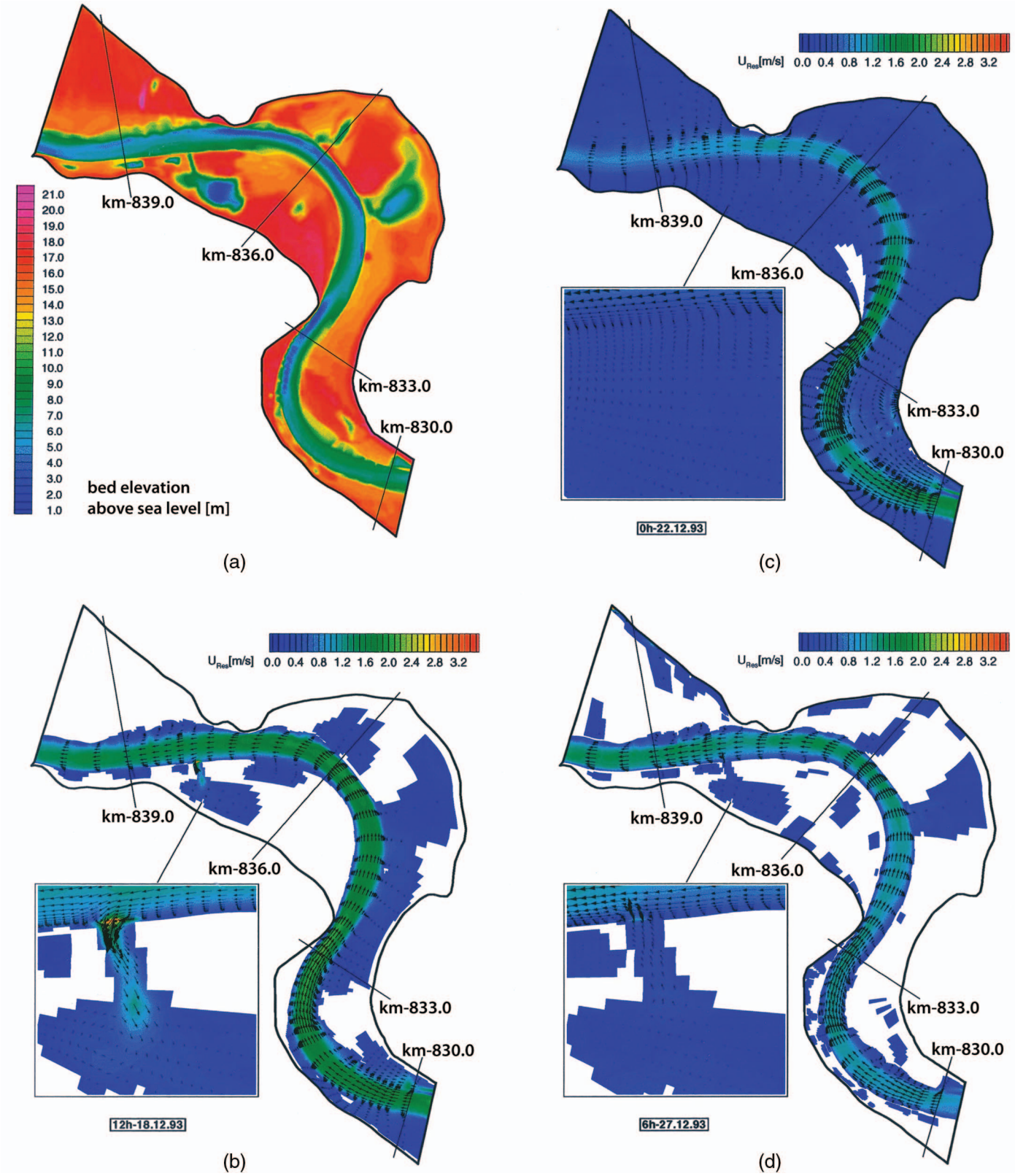

Fig. 5. (Color) Depth-averaged calculations of flood event in Rhine River near Vynen-Rees, depth-averaged velocity and flooded areas (adapted from Minh Duc 1998): (a) bed topography; (b) rising; (c) peak; (d) falling

East and West Germany. This stretch was in poorly maintained condition so that the BAW had the task of improving the conditions. They carried out field and laboratory measurements that were supported by various 2D and 3D calculations. The calculations were very challenging because of the complex geometry, including a sharp bend and many groynes on each bank of the river. Here results are presented of Fang's (2000) 3D simulations of a low-water discharge situation investigated by the BAW in a laboratory model, using a combined k-ε flow and sediment transport model developed by Wu et al. (2000). Simulations and experiments started

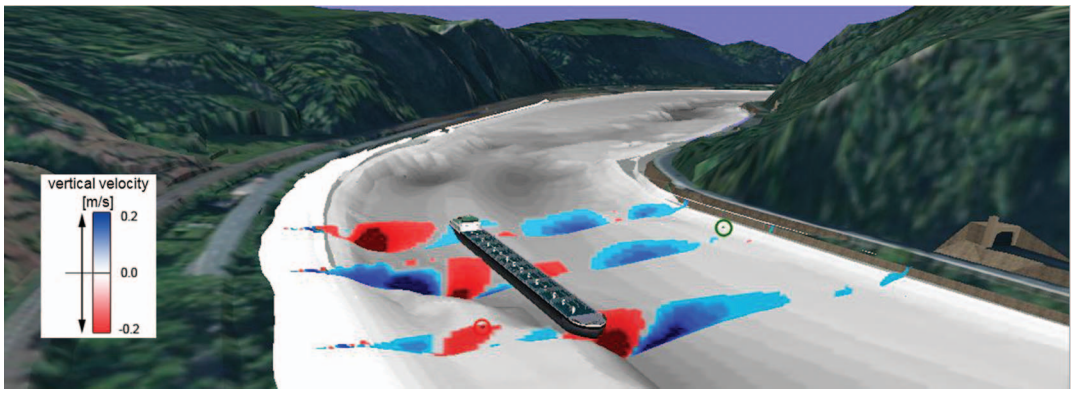

Fig. 6. (Color) Calculated vertical velocity in Rhine River near Loreley at location of barge accident (reprinted from from Wenka et al. 2016, with permission of Springer)

from a flat mobile bed and continued until an equilibrium state had evolved. Predicted and measured bed morphology at this state are compared in Fig. 7. There is general agreement about the results, with point bars and scour channels forming in the curved section. Bed-level and surface-velocity profiles are compared in Fang (2000) and also exhibit good quantitative agreement. This example shows that 3D models of the kind used can produce realistic answers for complex river-flow situations in practice.

An example is now presented from the field of wastewater treatment. Lakehal et al. (1999) calculated the flow and sludge concentration behavior in a secondary clarifier whose geometry and loading conditions are typical for tanks used in the Netherlands. The 2D (axisymmetric) simulations in the circular tank were carried out with the k-ε model, including buoyancy effects and a rheological model for the sludge blanket forming at the bottom of the tank. The evolving sludge-concentration distribution displayed in Fig. 8(a) shows clearly the sludge blanket at the bottom and the clear water above it flowing out of the tank. The complex flow evolving in the tank with various recirculation regions and strong stable stratification is illustrated in Fig. 8(b). Calculations of this type are nowadays used in the design of improved wastewater treatment systems.

The last example demonstrates that RANS models employed in unsteady mode can simulate situations with large-scale unsteadiness. Paik et al. (2004) performed 3D URANS simulations with the standard k-ε model for flow around a bundle of four bottom-mounted rectangular piers. Fig. 9(a), which in slightly different form was on the cover of the *Journal of Hydraulic Engineering* for many years, shows predicted instantaneous 3D stream traces depicting large-scale vortical structures evolving. Fig. 9(b) displays instantaneous velocity contours at one time instant. Clearly, the large-scale instabilities of the shear layers emanating from the bluff obstacles and the asymmetric vortex shedding could be reproduced. Fig. 9(b) also exhibits the (symmetric) time-averaged velocity contours, and Paik et al. (2004) report good agreement of the predicted streamwise mean velocity with experiments.

Two further examples of RANS calculations will be given in the section on LES, where they will be compared with results obtained by the LES method.

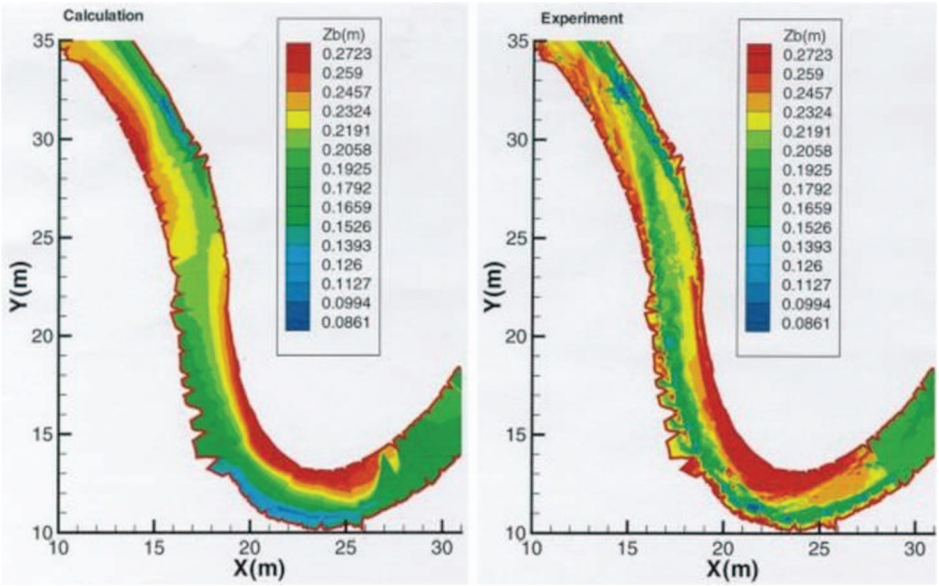

Fig. 7. (Color) Comparison of calculated and laboratory measurement of bed morphology of Elbe River (adapted from Fang 2000)

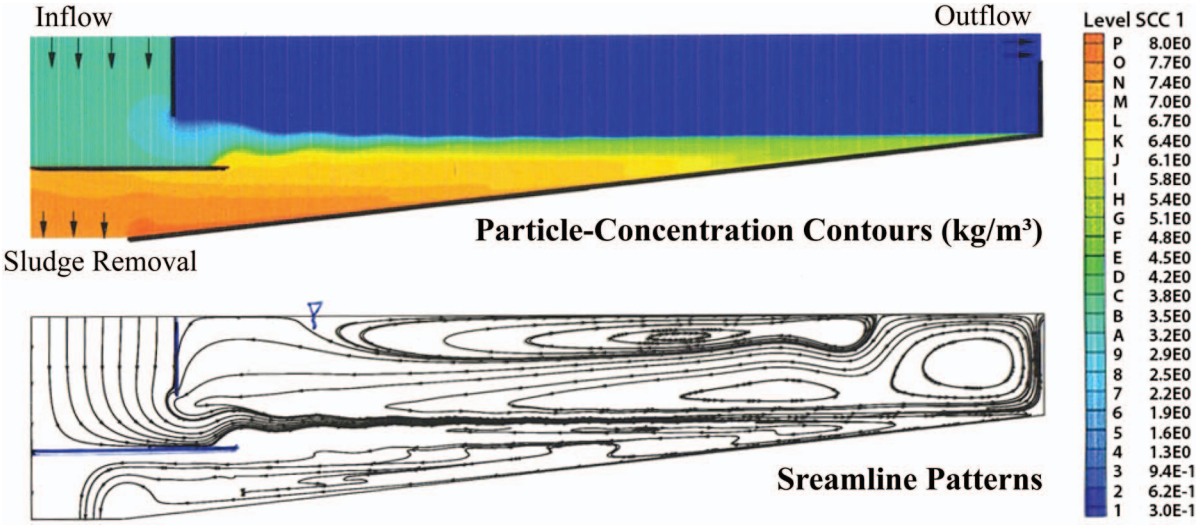

Fig. 8. (Color) Calculated particle concentration and streamlines in secondary clarifier (adapted from Lakehal et al. 1999, © ASCE)

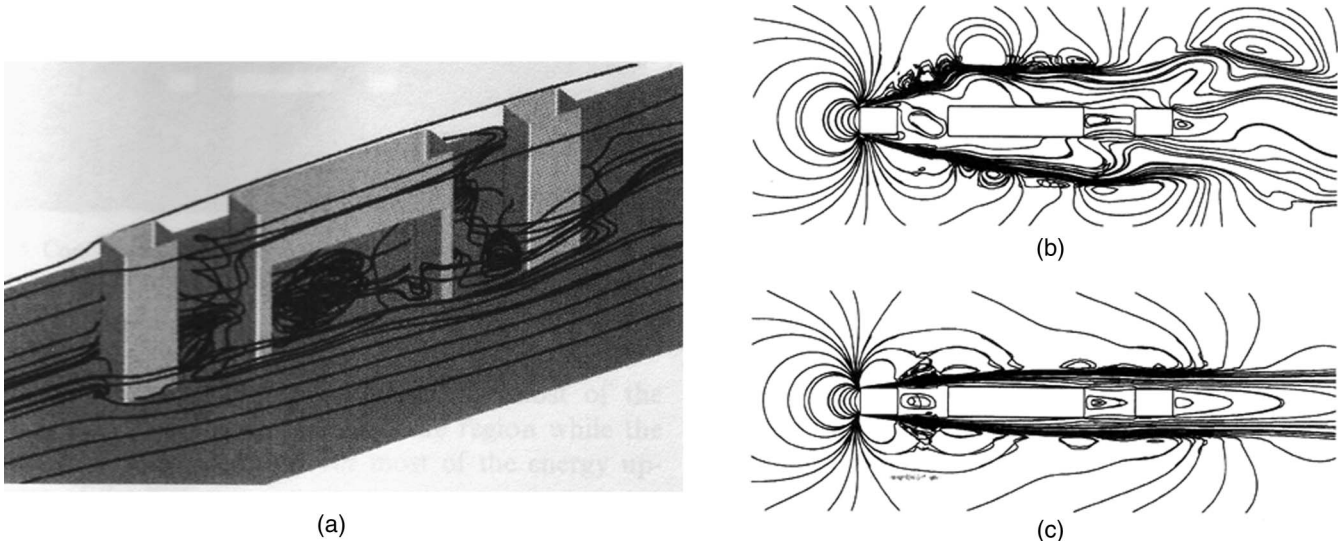

Fig. 9. URANS calculation of flow past group of bottom-mounted piers (reprinted from *International Journal of Heat and Fluid Flow*, Vol. 25, Issue 3, Joongcheol Paik, Liang Ge, and Fotis Sotiropoulos, "Toward the simulation of complex 3D shear flows using unsteady statistical turbulence models," pp. 513–527, Copyright 2004, with permission from Elsevier): (a) instantaneous 3D stream traces; (b) instantaneous velocity contours; (c) time-averaged velocity contours

Direct Numerical Simulations

As was mentioned at the beginning of the RANS section, the original time-dependent 3D Navier-Stokes equations govern the turbulent fluctuating motion in all details. However, they are not amenable to an analytical solution and can only be solved numerically. In the early 1970s, computer power became strong enough and numerical methods sufficiently developed to allow such solutions to be attempted for very simple problems. This was the beginning of the age of direct numerical simulations, a method in which the original Navier-Stokes equations are solved without any model assumptions. It is thereby necessary to resolve all scales of the turbulent motion, from the large, energy-containing scales to the smallest scales where dissipation takes place. This causes a resolution problem and serious restrictions on the applicability of the DNS method. The reason lies in the fact that the ratio of the largest scales L, which are of the order of the size of the flow domain, to the smallest scales η (the Kolmogorov scale) increases as $\mathrm{R}^{3/4}$. For a resolution of the smallest eddies, the mesh size of the numerical grid (in each direction) has to be of the order of η so that the number of required grid points increases as $\mathrm{R}^{9/4}$. As the time step in a time-advancing numerical calculation has to be decreased inversely with the mesh size, the number of floating-point operations (FLOPs) for a DNS was estimated to increase roughly as R^3. A detailed discussion on these estimates can be found in Reynolds (1990) and Pope (2000).

A review of the work in DNS until about 1997 was given by Moin and Mahesh (1998), who also described the origins and early history of DNS. The first DNS was Orszag and Patterson's (1972) computation of isotropic turbulence (grid turbulence) at a Reynolds number R_λ (based on Taylor micro scale λ) of 35 using 32^3 (= 32,768) grid points. In fairly recent calculations of the same flow

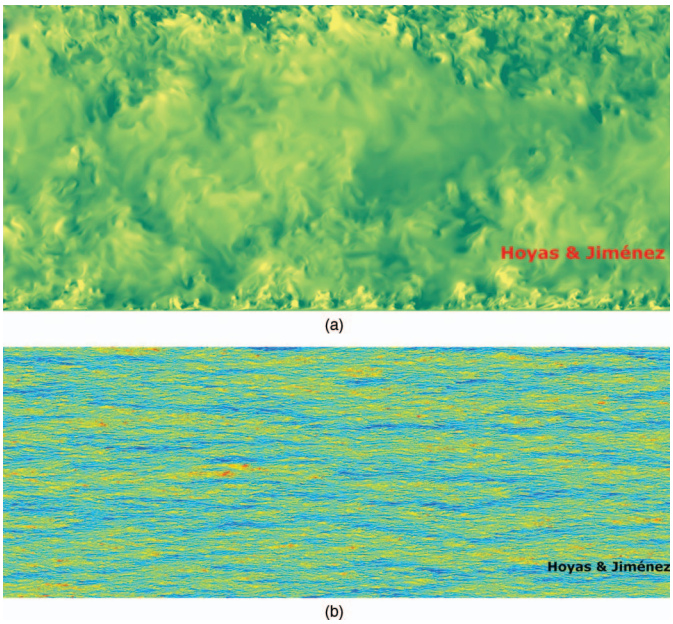

Fig. 10. (Color) DNS of closed-channel flows at $\mathsf{R} \approx 43{,}000$ [reprinted from Hoyas and Jiménez (2006a), with permission from Sergio Hoyas; related to Hoyas and Jiménez (2006b)]: (a) structures in vertical bottom-to-top plane visualized by wall-normal velocity component; (b) high- and low-speed streaks in horizontal plane near wall visualized by streamwise velocity fluctuations

by Ishihara et al. (2009), the Reynolds number could be pushed up to $\mathsf{R}_\lambda \approx 1{,}200$ by using $4{,}096^3$ ($\approx 68 \times 10^9$) grid points. This was possible because of a more than 10^6-fold increase in computer speed (Fig. 20). Of greater interest to hydraulics are calculations of channel flow. The first DNS of closed-channel flow was reported by Kim et al. (1987) for an R of 3,300 using 2×10^6 grid points. Here R is based on bulk velocity and channel half-width, which corresponds to channel depth for open-channel flow. With increasing computer power, channel-flow simulations with ever-increasing R were carried out over the years, and at the time of writing, the largest calculation is that of Lee and Moser (2015) at $\mathsf{R} = 125{,}000$. This employed 242×10^9 grid points and ran for several months on the Peta-FLOP/S computer Mira. This shows the enormous computing effort necessary for DNS, even for simple flows, which precludes its use for practical calculations in the foreseeable future. However, DNS has become an important and very useful tool in research as it allows the extraction of all details of the turbulent motion and hence the study of the basic mechanisms of this complex motion. Many studies on the structure of turbulence based on DNS results have been reported (e.g., Lozano-Duran and Jimenez 2014), and examples of such visualizations of structures are given in Fig. 10 taken from the plane-channel flow DNS of Hoyas and Jimenez (2006a, b) at $\mathsf{R} \approx 43{,}000$. Fig. 10(a) shows the turbulent structures from the top wall to the bottom wall visualized by the wall-normal velocity component, revealing fairly large structures in the channel center and much smaller ones near the walls. Fig. 10(b) depicts the structures in a plane close and parallel to the wall illustrating the streaky nature of turbulence near walls. As described in Nezu and Nakagawa (1993), near-wall turbulence also exhibits hairpin vortices, and these are shown in Fig. 11, extracted from a DNS of a turbulent boundary layer by Wu and Moin (2009). DNS has also provided much useful information on statistical quantities, especially those that are difficult to measure, such as the dissipation rate ε.

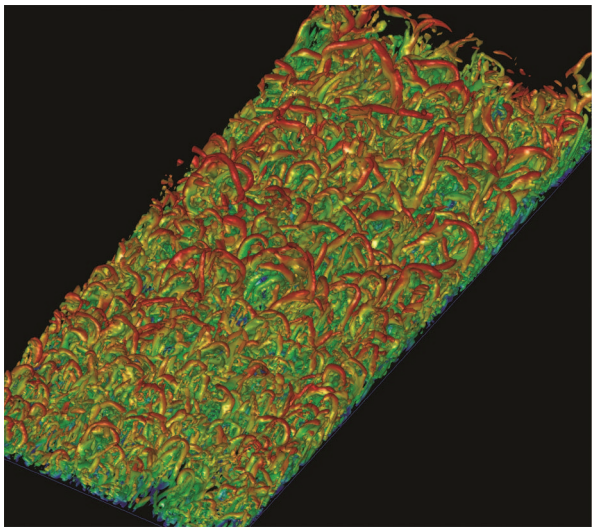

Fig. 11. (Color) Hairpin vortices near wall from DNS of a flat-plate boundary layer (reprinted from Wu and Moin 2009, with the permission of AIP Publishing)

Fig. 12. DNS of instantaneous streamlines at free surface of open-channel flow (reprinted from Pan and Banerjee 1995, with the permission of AIP Publishing)

Open-channel flow was also calculated by DNS, with a focus on the turbulent processes at and near the free surface. A typical study of this kind is that of Pan and Banerjee (1995) at $\mathsf{R} = 6{,}700$. Fig. 12 shows the predicted streamlines at the water surface, exhibiting regions with upwelling attributable to impinging bursts, downdrafts in between, and also attached (nearly vertical) vortices at the edges of the upwelling. The complex turbulent processes, which can be studied in detail with the aid of DNS results, have a governing influence on the gas transfer at the surface. The latter, or rather heat transfer as its equivalent, was simulated using DNS, e.g., by Yamamoto et al. (2001). In this study for $\mathsf{R} = 3{,}200$ and Prandtl numbers (representing the heat diffusivity) of 1 and 5, extensive statistics are reported as well as visualizations of coherent structures and scalar fields. In gas transfer problems the Schmidt number Sc representing mass diffusivity is usually large ($\approx$500 for oxygen). As a consequence, the near-surface concentration boundary layer, where molecular diffusion takes place, is very thin (10–1,000 μm), requiring an especially high resolution in a DNS. Herlina and Wissink (2014) performed gas-transfer DNS for various Sc values up to 500. In these DNS, however, there was no mean flow and the turbulence penetrating to the surface was hence not bed-generated but artificially-generated grid turbulence. Fig. 13 shows predicted concentration contours near the surface superimposed with velocity vectors of the turbulent motion for two values

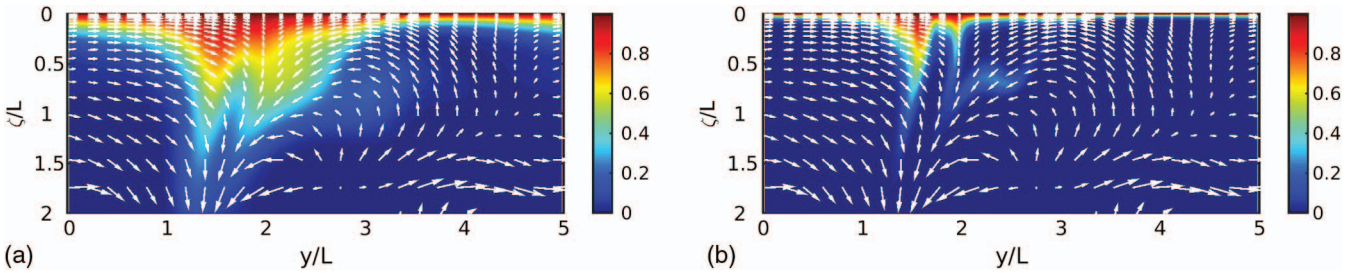

Fig. 13. (Color) DNS of scalar transport across free surface; instantaneous scalar concentration contours and velocity field near surface (courtesy of H. Herlina, with permission; adapted from Herlina and Wissink 2014): (a) $Sc = 2$; (b) $Sc = 32$

of Sc, illustrating the interplay between turbulence with the scalar field. In regions of upwelling, low-concentration fluid is pushed to the surface so that the concentration layer there is thin. In regions with downdraft, excursions of high-concentration fluid further down into the water prevail. The layer with higher concentration is considerably thinner in the case with higher Sc. In this context, it should be mentioned briefly that situations with gas bubbles (in vertical channel flow) have also been calculated by DNS (Santarelli et al. 2016).

The channel flow DNS discussed so far were all for smooth walls. Fairly extensive DNS have also been carried out with one wall being rough. Ikeda and Durbin (2007) report a very comprehensive and detailed study of such flow at $\mathsf{R} = 6{,}520$ with rectangular ribs of dimensionless roughness height $k^+ = 110$, which corresponds to a fully rough case. Statistics of interest and visualizations of turbulence structures are provided so that the study gives a good insight into the turbulence mechanics in the vicinity of roughness elements. Similar DNS were carried out by Burattini et al. (2008) and Leonardi et al. (2007) for R in the range 2,800–13,000 and different distances of rib elements. The emphasis here was on statistical quantities, in particular the shift Δu^+ of the log law attributable to roughness.

Chan-Braun et al. (2011) calculated channel flow with a layer of packed spheres as roughness elements. The roughness height $k^+ = 49$ was in the transitionally rough regime. Apart from studying the details of the turbulence in the vicinity of and between the spheres, the unsteady forces and torque acting on the spheres from the turbulent motion around them were determined and analyzed, and also with respect to their timescale and length scale (Chan-Braun et al. 2013). This is a direct precursor study for simulating the erosion of sediment particles. Such a simulation, coupling the DNS with a particle collision model, was carried out by Vowinkel et al. (2014, 2016), who introduced mobile spherical particles into open-channel flow ($\mathsf{R} = 2{,}541$) with a layer of fixed spheres as roughness elements on the bed. For a Shields number below the critical one, most mobile particles settled in a second layer above the fixed spheres, but occasionally particles were eroded from this layer. These erosion events were studied in detail, thereby unveiling the mechanism of the initiation of particle motion attributable to the combined effect of hydrodynamic and contact and collision forces. The study revealed that it was primarily sweep events that initiated the particle motion, but collisions also had a triggering effect. Kempe et al. (2014) studied the collision model in detail, as well as the bed-load transport and the formation of sediment patterns for a trans-critical Shields number.

Kidanemariam and Uhlmann (2014) went one step further and simulated the formation of ripples and dunes by coupling a DNS with a collision model, i.e., without any model for the flow and the particle-flow interaction. Follow-up calculations (Kidanemariam 2015) were carried out for open-channel flow at $\mathsf{R} = 6{,}000$, starting from a flat mobile bed consisting of a thick layer of about 1 million particles and using about 10^9 grid points for the grain resolving simulation. Fig. 14(a) exhibits in top view the formation of bed patterns and Fig. 14(b) gives a side view after dunes had been formed, showing the deformed bed, particles in motion, and instantaneous spanwise vorticity illustrating the turbulence structures. All details of the interaction of turbulence and sediment particles and hence the basic mechanism behind sediment transport can be studied by such calculations, but it is clear that the method is far too expensive for application in practice. The next section will show that bed formations can also be simulated by LES, and for higher R and more complex configurations closer to practice. The difference from the DNS presented here is that in the LES reported there, a morphodynamic model is coupled to the

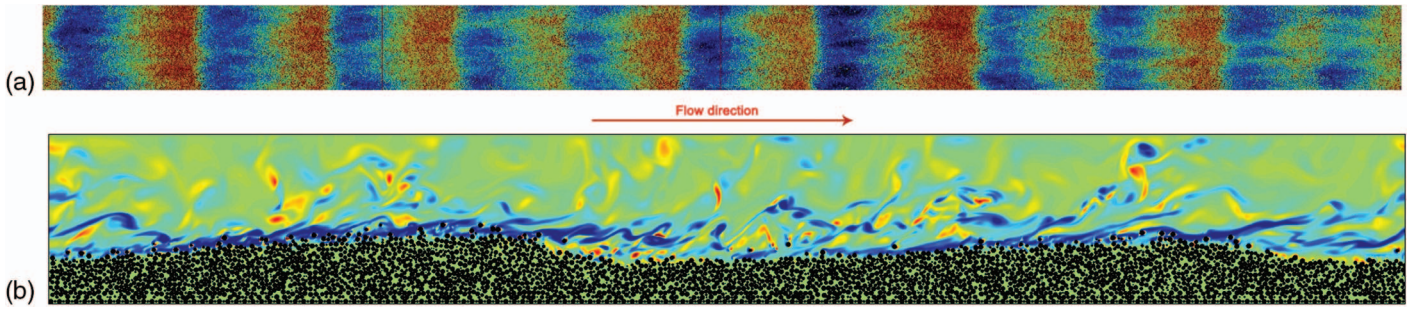

Fig. 14. (Color) DNS of flow and particle movement leading to dune formation in channel flow with thick mobile bed: (a) top view of particle positions after dunes have developed, colored by vertical location (courtesy of A. Kidanemariam, with permission; based on Kidanemariam 2015); (b) side view of deformed bed, particles in suspension and turbulent structures visualized by spanwise vorticity (reprinted from Kidanemariam 2015, with permission)

LES to handle the interaction of the sediment with the turbulent flow.

All DNS of free-surface flows presented here and all LES examples in the next section, except that in Fig. 18, treated the free surface as a fixed-plane zero-shear-stress surface (rigid-lid approximation). This treatment was discussed by Rodi et al. (2013).

Various free-shear flows (mixing layers, jets, wakes) were also calculated by DNS (e.g., Moin and Mahesh 1998). The far field is difficult to resolve at Reynolds numbers of interest and is more amenable to LES. The near field of wakes behind circular cylinders was investigated up to $R = 10{,}000$ (Dong et al. 2006; Wissink and Rodi 2008), and the details of the complex flow with vortex shedding could thereby be studied. A larger number of further DNS of flows relevant to hydraulics have been conducted, which cannot all be reviewed here. A fairly recent review of DNS with a very large collection of references was provided by Alfonsi (2011).

Large-Eddy Simulations

Because resolving the small-scale dissipative motion in a DNS becomes prohibitively expensive at larger R, a method was devised that resolves in 3D unsteady calculations on an affordable grid only the eddies larger than the mesh size, but accounts for the unresolved small scales through a subgrid-scale (SGS) model. This is the large-eddy simulation method that lies between the DNS and RANS approaches. The idea and advantage of LES is that the large-scale, energetic motion depending on the boundary conditions does not need to be modeled as in the RANS method, and that the small-scale motion does not need to be resolved and is easier to model since it is more universal. The concept is outlined in more detail in the book of Rodi et al. (2013), in which also the equations are given and the most common SGS models are described. In contrast to the RANS method, in which the original Navier-Stokes equations are time averaged, in LES the equations are spatially filtered corresponding to spatial averaging. In effect, the quantities solved for are averages over mesh cells of the numerical grid. The filtering/averaging introduces stresses/fluxes attributable to the unresolved fluctuations, which need to be determined by a SGS model. Most LES have been carried out with an eddy-viscosity SGS model. The governing equations are then formally identical to URANS equations based on an eddy viscosity, but the eddy viscosity ν_t is much smaller in the LES case. ν_t is now related to quantities of the unresolved small-scale motion, the length scale of which is given by the user-specified mesh size while in RANS methods the characteristic length scale has to be determined by the turbulence model. As a consequence, LES are not grid independent; with continuous refinement of the grid, the SGS viscosity becomes smaller and smaller and the LES finally turns into a DNS. A detailed discussion on the similarities and differences between the URANS and LES approaches is given in Rodi et al. (2013).

The fact that the small-scale motion does not need to be resolved reflects of course on the computational cost. For flows remote from walls, this cost is virtually independent of R (Pope 2000), but in general it is still considerably higher than for RANS/URANS. For wall-resolved near-wall flows, the number of grid points required depends on R and was estimated to increase as $R^{1.8-2.0}$ (Chapman 1979; Baggett et al. 1979).

LES was invented in the 1960s by meteorologists (Smagorinsky 1963) aiming at the simulation of large-scale motions dominating the flow in the atmosphere. The first application to an engineering flow, namely plane-channel flow at high R, was also carried out by a meteorologist (Deardorff 1970). Soon after, engineers adopted the method and developed it further with application to channel flows of various kinds (Schumann 1975; Grötzbach 1979). Toward the end of the 1970s, a group at Stanford University took the lead in the development and application of LES. Then groups in other countries where powerful computers were available like France, England, and a little later Japan joined the research in LES. The first calculations were for fairly simple flows (homogeneous turbulence, channel flow) but were gradually extended to more and more complex flows. As the availability of powerful computers became more widespread, so did the work on LES, which saw a strong increase in the 1990s all around the world. Again this development took place primarily in the area of mechanical/aerospace engineering. By now, research in LES and hybrid LES/RANS methods has clearly overtaken that in RANS modeling. The LES and hybrid methods are now available in most general-purpose commercial CFD codes and are already used for solving practical problems. Galperin and Orszag (1993) gave an overview of the early history of LES and the range of applications until about 1990. A larger number of books and review articles on LES not geared to hydraulics is now available and cumulatively cited (and hence not repeated here) in Rodi et al. (2013) and Stoesser (2014), and a projection of the state of the method by 2030 and beyond was recently published by Piomelli (2014).

The first 3D LES of aquatic flows was probably carried out by Bedford and Babajimopoulos (1980) for the Great Lakes. It then took some time before hydraulic engineering problems were tackled by LES, starting in the 1990s, but still at a low pace, and it was only in the mid-2000s that a sharp increase in the use of LES in hydraulics began. Stoesser (2014) counted 50 LES studies that were published during 2009–2013 in the main hydraulics journals. At the instigation of the IAHR, Rodi et al. (2013) produced a monograph on LES in hydraulics that introduced the method in a manner geared to hydraulic and environmental engineers. They also summarized the experience gained in the field by 2013 as well as the potential and requirements of the method. Stoesser (2014) complemented this monograph by extending the review and providing an outlook on where LES in hydraulics will go and what the research challenges are. The book by Rodi et al. (2013) covers the various facets of LES so that these need not be dealt with again here in detail and it suffices to highlight a few key elements. A variety of SGS models have been developed and tested. The main ones used in hydraulics calculations are the Smagorinsky (1963) model, which in analogy to the RANS mixing-length model relates ν_t to the gradients of the resolved velocity, and the dynamic version of this that determines the model parameter from information available from the smallest resolved scales. Experience has shown that the SGS model adopted is not very critical as long as a reasonably fine grid is used (Stoesser 2014). The LES results are more sensitive to the treatment of the boundary conditions—also called supergrid modeling (Stoesser 2014)—such as the inflow conditions, the free-surface conditions, and the wall conditions, where handling of roughness is of particular relevance. Various possibilities exist for the treatment of walls that have a large effect on the computing cost. Wall-resolving LES need to be quasi-DNS near the wall where they require a very fine grid—this must be fine enough to resolve the dominating turbulent structures there, including the streaks shown in Fig. 10(b). These structures become smaller as R increases so that the estimated number of grid points increases as $R^{1.8-2.0}$, as mentioned before. Such wall-resolving calculations are therefore not feasible for high R situations occurring in practice.

There are various less costly alternatives for treating the near-wall region in LES. One uses wall functions to bridge this region, and various such functions are available. The other employs a hybrid LES/RANS method in which the near-wall region is resolved with a more economical RANS (actually URANS) model and only

the region remote from the wall by LES. A variety of such models are available (Rodi et al. 2013). Perhaps the most popular one, also used in hydraulics, is the detached eddy simulation (DES) of Spalart et al. (1997). This employs the Spalart and Allmaras (1994) eddy-viscosity model as a RANS model near walls and as a SGS model farther away. The switch occurs when the length scale from the RANS model (basically the wall distance) becomes larger than the grid size. Hybrid models are also useful in the form of embedded LES where only a subdomain with particularly complex flow (e.g., around structures) is calculated by LES but the rest by a more economical RANS model (Rodi et al. 2013). For practical calculations in hydraulics, the future is seen to belong to hybrid methods, as pure LES will mostly be too expensive.

Two-Dimensional Depth-Averaged LES

In shallow water flows with a two-range spectrum (Fig. 4), 2D LES can be taken into consideration in which only the large-scale horizontal 2D eddies are resolved directly while the effect of 3D turbulence with scales smaller than the depth is modeled. The governing 2D equations are obtained by depth-averaging the 3D LES equations. The former are the same as the DA RANS equations discussed in the RANS section when used in unsteady mode, but the resolved horizontal large-scale motions are in this case considered to be unsteadiness of the mean flow rather than turbulence. Hinterberger et al. (2007) discussed this connection between the two approaches in some detail. In both, the depth-averaging leads to the appearance of a bed-friction term and DA horizontal turbulent fluxes. When the 2D horizontal eddy motion is well resolved, these fluxes are entirely the result of the 3D bed-generated turbulence and are usually determined with the sub-depth-scale model of Elder (1959) introduced previously. When the horizontal motion is not sufficiently resolved, a subgrid-scale model also must be used, e.g., of the Smagorinsky (1963) type.

Unsteady DA calculations have been carried out quite early (Leendertse 1967; Kuipers and Vreugdenhil 1973), but were not called DA LES. The effect of small-scale 3D turbulence was thereby primarily accounted for by a model for the bed friction and some numerical viscosity. Later, calculations also included the Elder model and often additional viscosity/diffusivity accounting for (nonturbulent) dispersion effects (see discussion in RANS section). The DA LES approach is used in practical calculations, e.g., by BAW, and also with the *DELFT3D* code, involving the Smagorinsky (1963) model, in the latter case with the special version of Uittenbogaard and van Vossen (2004).

Hinterberger et al. (2007) calculated various laboratory shallow water flows (mixing layer, flow past cylinder, and in groyne fields) with 2D DA LES and compared the results with those from 3D LES. The results were found to be mostly reasonable but not as accurate as those from 3D LES. These authors as well as Uijttewaal and van Prooijnen (2004) found that for situations where large horizontal eddies are not generated by topographical forces such as those behind structures, but by the bed-generated 3D turbulence attributable to the so-called backscatter effect, special source terms need to be introduced into the DA equations to yield such eddies.

Application Examples

The book of Rodi et al. (2013) presents many application examples of LES calculations, covering a wide variety of hydraulic flows, including the fundamental ones, and Stoesser (2014) cited further recent applications. Hence, here only a few *additional* 3D LES application examples are presented. The first concerns tandem cylinders in open-channel flow calculated by AlQadi et al. (2015) with a commercial CFD code. A very complex flow develops because of the interaction of the two cylinders with each other and with the bottom and the free surface. This was analyzed in detail with the aid of the LES results, and the statistical quantities were compared with laboratory measurements and found to be in good agreement. Fig. 15 gives a 3D view of the resulting flow structures visualized by the λ_2 criterion (Rodi et al. 2013), revealing primarily the fine-scale structure. The horseshoe vortex wrapping around the front cylinder can be seen as well as the shear layer separating from this, rolling up into 2D vortices and breaking up into hairpin-type vortices. The color coding with velocity shows reverse-flow regions behind both cylinders and high velocity on their sides.

In the next two examples, results from LES are compared with RANS calculations. The first concerns flow in a naturallike meander investigated experimentally in the Outdoor StreamLab (OSL) of the St. Anthony Falls Laboratory. On the same grid, Kang and Sotiropoulos (2012) performed LES (dynamic Smagorinsky model) and RANS (with the SST model of Menter 1994) calculations. Both models predict the gross features of the flow reasonably well, but only LES manages to reproduce certain key features of the complex flow in the bend, such as the appearance of two counter-rotating secondary-flow cells and of a horizontal recirculation eddy over the point bar on the inner bank. This difference is brought out clearly in Fig. 16 displaying the secondary motion and streamwise velocity contours together with the bathymetry at various cross sections. The RANS method fails primarily in regions with strong turbulence anisotropy, a phenomenon that LES copes with well.

In work aimed at improving lock design, BAW (Thorenz 2009) calculated the flow in the lower approach area of a lock and in the associated stilling basin with both LES (Smagorinsky SGS model) and a RANS method ($k-\varepsilon$ model). Fig. 17 shows the configuration with openings at the left of the basin through which water can be pumped or discharged. This water can exchange freely with that in the main lock area. Of primary interest in this computational study was the effect of this exchange flow on the ships in the lock. The simulations were carried out for a case with unsteady discharge

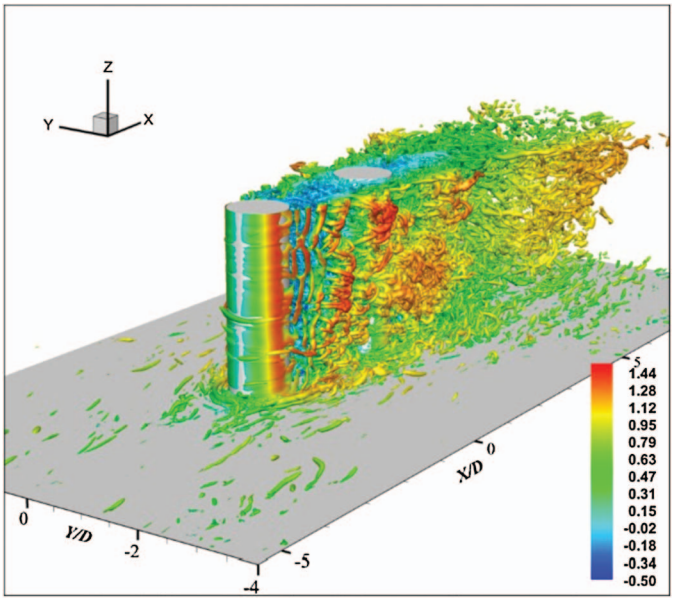

Fig. 15. (Color) LES of flow past tandem cylinders placed in open channel; visualization of structures by λ_2 criterion, colored by streamwise velocity (reprinted from AlQadi et al. 2015, with permission of Springer)

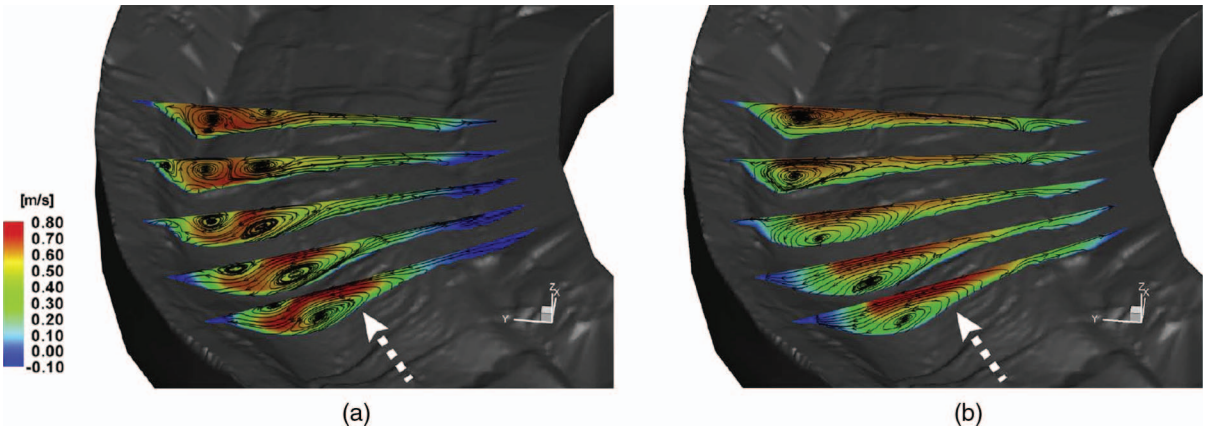

Fig. 16. (Color) Calculated secondary flow streamlines and contours of streamwise velocity in meander (reprinted from Kang and Sotiropoulos 2012, with permission from John Wiley & Sons Ltd.): (a) LES; (b) RANS

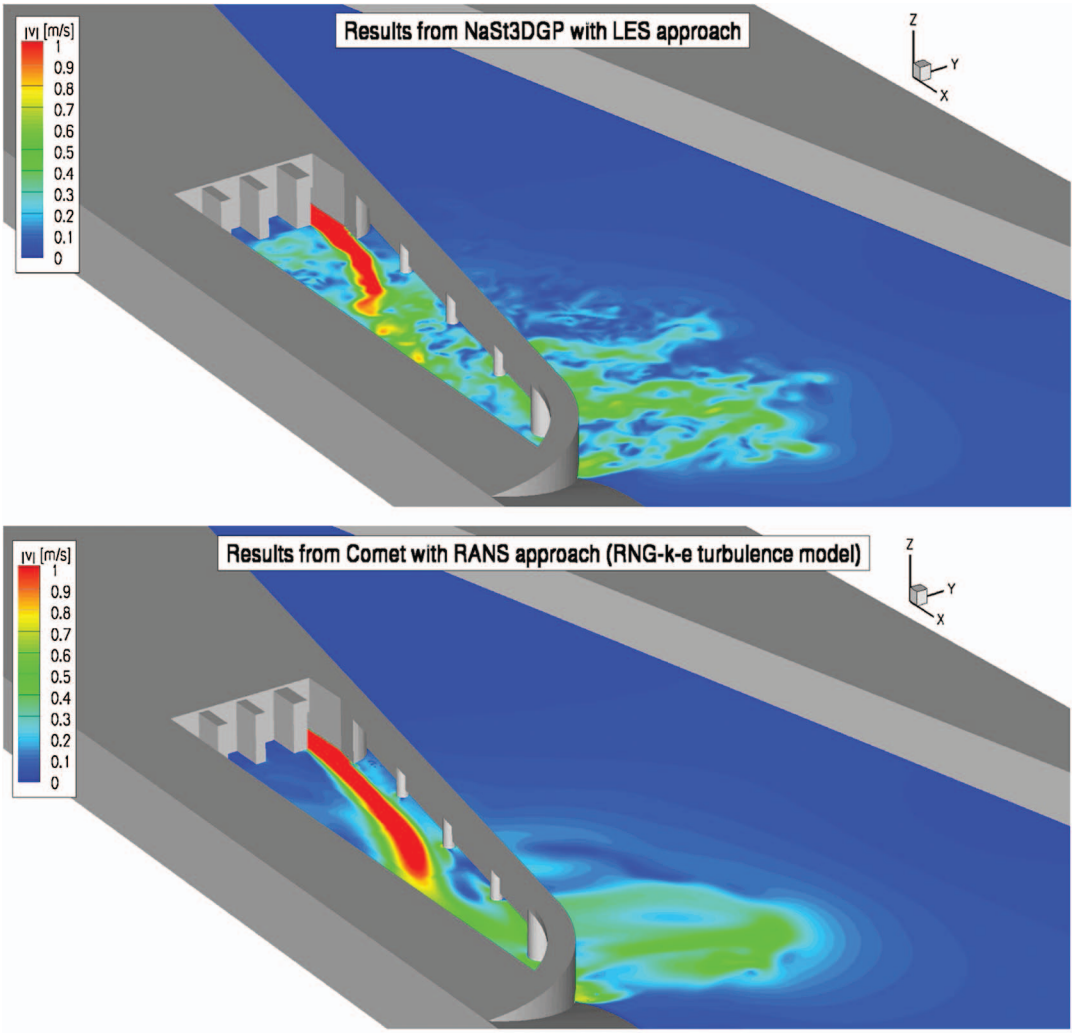

Fig. 17. (Color) Calculations by LES and RANS of flow in lower approach area of a lock: instantaneous velocity in a submerged horizontal plane (courtesy of C. Thorenz, with permission)

from one of the openings. Fig. 17 shows the calculated velocity at one instant in a submerged horizontal plane. The large-scale flow field obtained with the two methods can be seen to be similar, but the LES also yields the smaller-scale motion, the fluctuations of which may be relevant for boats that also use the lock.

Fig. 18 shows recent LES by Chua et al. (2016) of open-channel flow over bed-mounted square bars at intermediate submergence and wide bar spacing. In this case, the flow separating at the bars reattaches on the bottom between the bars and a hydraulic jump develops at the free surface, which was computed and tracked

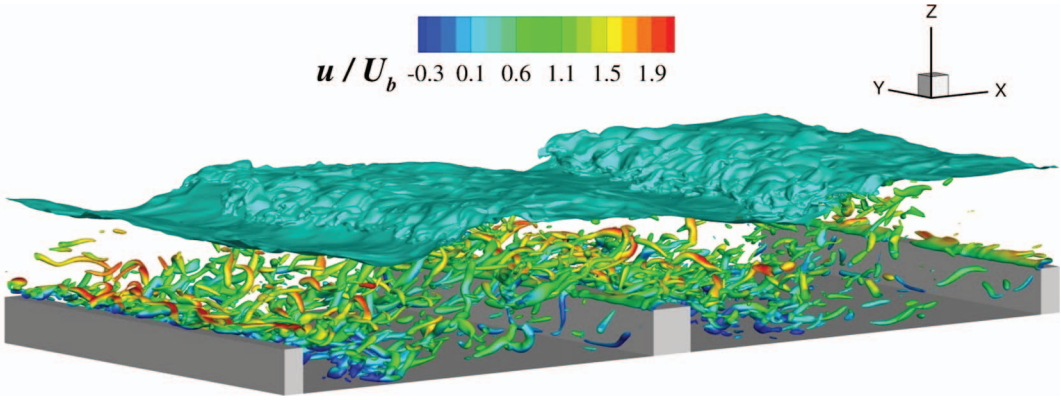

Fig. 18. (Color) LES of open-channel flow over bed-mounted square bars; visualization of flow structures by the Q criterion, colored by streamwise velocity (courtesy of T. Stoesser, with permission; related to Chua et al. 2016)

with the level-set method. In the figure, for one instant, the irregular position of the surface with hydraulic jump between the bars is visualized as well as the turbulence structures in the channel by the Q criterion (Rodi et al. 2013). The structures are colored by velocity, which clearly shows reverse-flow regions behind the bars, but also in front and on top. The flow separates at the leading edge of the bars, forming coherent spanwise vortices that then disintegrate into smaller hairpin-type vortices. Coherent structures are also generated at the hydraulic jump; they are convected downstream and merge with the structures originating from the separated shear layer behind the bars. The very complex flow field in this case can be studied in detail with the aid of the LES results.

The last LES application example concerns sediment-transport calculations by Sotiropoulos and Khosronejad (2016) of the formation and migration of sand waves as studied experimentally in an open channel by Venditti and Church (2005). In these calculations, LES employing wall functions was coupled with a morphodynamic model based on the Exner equation and on sediment-entrainment and bed-load-flux relations that are empirically correlated to the bed shear stress. Hence, this approach is fundamentally different from the one discussed in the DNS section (e.g., relating to Fig. 14) where particle-flow interaction was directly resolved. Such an approach with resolution of the flow around each grain would be difficult with LES as a near DNS would still be necessary in the vicinity of the moving particles. LES were performed in the context of Lagrangian models using point particles. The hydrodynamic forces acting on these were expressed through drag and lift coefficients (e.g., Escauriaza and Sotiropoulos 2011; Schmeeckle 2014). The effect of the particles on the flow, if important, needs then to be accounted for by an extra model term in the LES momentum equations, and the effect of the unresolved turbulent motion on the particles ideally by a SGS model for the particle dynamics—but no such model seems to have been developed so far. Coming back to the calculations by Sotiropoulos and Khosronejad (2016), Fig. 19 shows simulated bed features after a certain time starting from a flat bed, in comparison with observed features. The results demonstrate that the development of very irregular 3D bed forms can be simulated realistically by this method. The method was also found capable of reproducing intermediate-scale dunes downstream of various rock structures observed experimentally in the Outdoor StreamLab of the St. Antony Falls Laboratory, while URANS calculations using the samemorphodynamic model failed to excite the evolving bed instabilities (Khosronejad et al. 2015). On the other hand, such URANS calculations could capture realistically the dune formation in large-scale meandering rivers for which LES-based methods would still be too

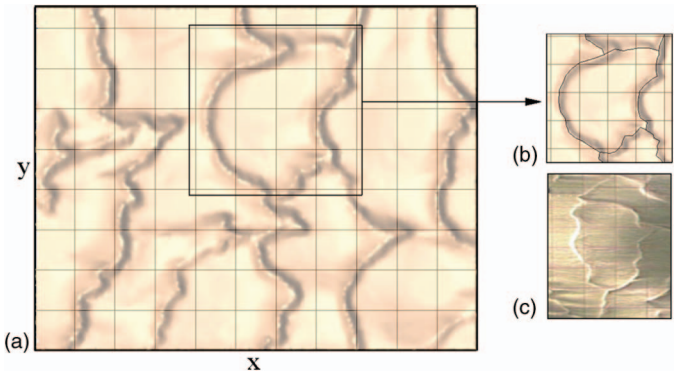

Fig. 19. (Color) Bed features forming in open-channel flow over mobile bed; comparison of (a and b) LES and (c) experimental observation (reprinted from Sotiropoulos and Khosranejad 2016, with the permission of AIP Publishing)

expensive. As shown in Fig. 7, such URANS calculations also yielded realistic bed deformations in the Elbe River.

Conclusions

A condensed review of methods for handling turbulence and its effects in hydraulic-flow calculations was presented from a historical perspective. The earliest methods were empirical relations treating turbulence only globally. They are still useful for solving simple problems and for providing first estimates, and they will continue to be employed for this by practicing engineers. They also play an important role in 1D integral (or layer) methods, which have a wider range of applicability.

Field methods based on the Reynolds-averaged Navier-Stokes equations are a much more powerful tool that came into use with the advent of the computer. These methods account locally for the effects of turbulence through a statistical turbulence model. They allow a detailed treatment of the flow and associated processes and calculations for virtually arbitrary geometries and hence for situations with complex irregular boundaries. The methods can cope with the interaction of different flow regimes and of different physical phenomena. With the proliferation of computers, RANS methods became more and more popular and are now used routinely in hydraulic engineering practice. The RANS models described briefly in this paper are implemented in commercial and open-source codes. The simpler and cruder ones are used for

large-scale far-field calculations, and the more refined ones for solving near-field problems. The continuing increase in computer power, together with the development of flexible and efficient numerical methods, enabled the computation of more and more complex situations and larger domains. RANS methods will continue to be the primary workhorse in practical hydraulic flow calculations for many years to come. The calculations will be carried out primarily with the models described above; more advanced models are available but never became popular in hydraulics, and not much research is now carried out in this area.

The RANS models commonly used reach their limits when turbulent transport by large-scale structures plays a dominant role and when turbulence exhibits strong anisotropy. In such situations, eddy-resolving methods are clearly superior, but they require considerably higher computing effort and hence have experienced wider use only since the 1980s. DNS, resolving eddies of all scales, is a very powerful method that has become an important research tool allowing the study of all details of turbulence, including those defying experimental study. The continuous growth of computing power allows the simulation of flows with higher and higher Reynolds number and more complex phenomena such as two-phase flow, particle-flow interaction, and so on. However, the computational effort required by DNS is enormous so that the method is not suitable for practical calculations in the foreseeable future.

LES is markedly cheaper as it resolves only the scales larger than the mesh size of a grid that can be afforded. The method took an enormous upswing in the last decades and emerged as having great potential. It is already incorporated in commercial and open-source codes and used in certain practical calculations. Its role in such calculations and in hydraulic research will grow as the computer power increases further. This is convincingly described in a recent vision paper of Sotiropoulos (2015) on hydraulics in the era of exponentially growing computer power—the latter is illustrated in Fig. 20 by showing the speed of top computers plotted versus the year when they were installed. The paper of Sotiropoulos further summarizes very well the potential of advanced simulation techniques such as LES (but also URANS) and the various areas and problems where they will bring a big step forward. The paper, as well as another vision paper by Stoesser (2014), point out where further research advances are necessary, and both conclude that this is the area of supergrid modeling, i.e., the modeling of boundary effects, such as inflow, free surface, rough walls, and the interaction with mobile beds. It is also clear from these two vision papers that pure, wall-resolving LES is not the method for use in practice but the employment of either wall functions or hybrid LES/RANS methods. Even though the advanced calculation methods have enormous potential, experimental studies will continue to play an important role in hydraulics for validating and complementing calculations, as well as in their own right.

The advancements in turbulent flow simulations and their applicability to situations with complex geometry and multiphysics phenomena relied heavily on significant advancements in numerical methods. This important element of simulation methods could not be covered at all in this review focusing on the handling of

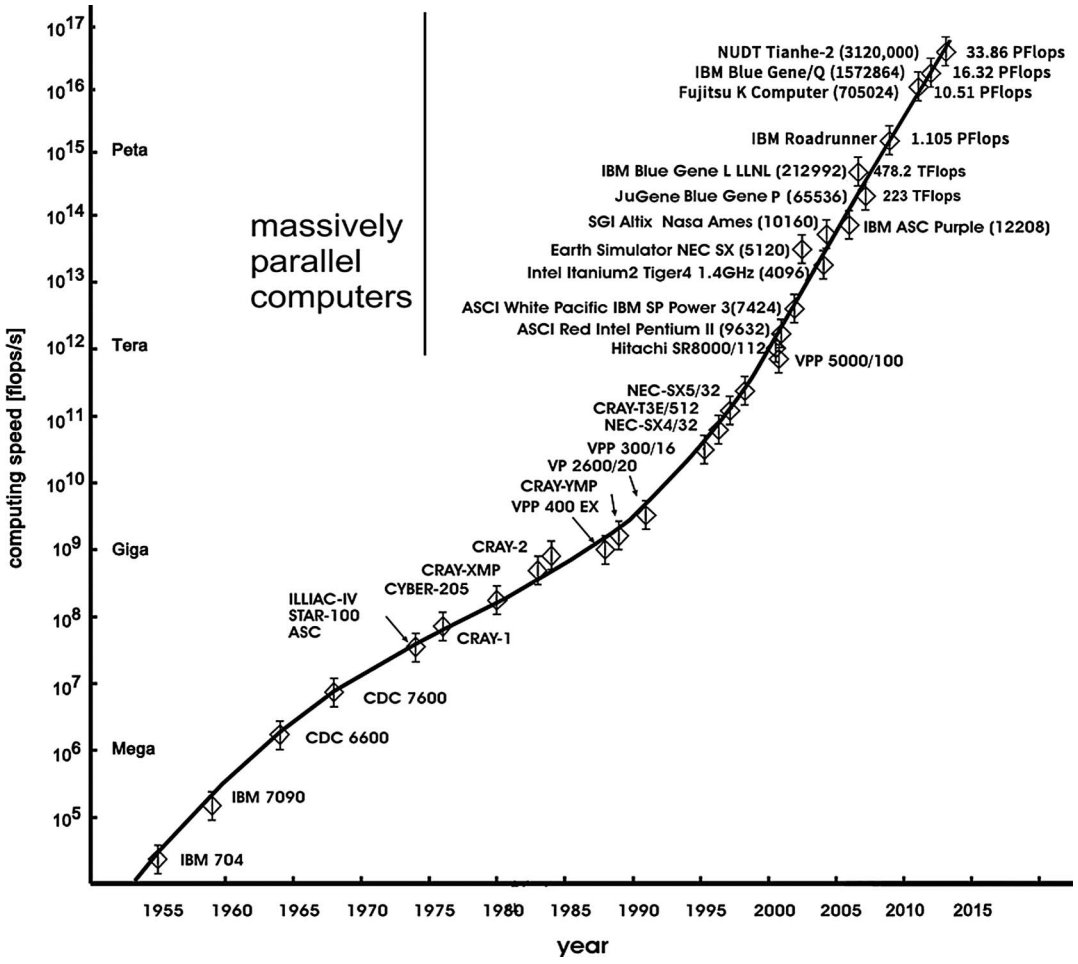

Fig. 20. Development of computer speed over the years

J. Hydraul. Eng., 2017, 143(5): -1--1

turbulence, so the reader is referred to the various research papers cited. New numerical approaches have been and are still being developed, and one has become popular in hydraulics, namely the meshless smooth particle hydrodynamics (SPH) method (Violeau and Rogers 2016), which however has not been used much for turbulent flows so far.

The treatment of turbulence in hydraulics calculations has gone a long way from Chezy and his simple friction law to the sophisticated DNS and LES methods, which allow the extraction of all details of the turbulent motion and the latter, especially in the hybrid LES/RANS version, the calculation of very complex real-life, multiphysics problems. The fascinating prospects of these methods will certainly bring excitement to the work of hydraulic researchers and practitioners in the years to come.

Acknowledgments

The author should like to thank H. Herlina, A. Kidanemariam, T. Stoesser, C. Thorenz, and T. Wenka for providing figures included in this paper. The author also thanks S. Wans for his help in the preparation of the manuscript as well as the Associate Editor and the reviewers for their constructive comments.

References

Alfonsi, G. (2011). "On direct numerical simulation of turbulent flows." *ASME Appl. Mech. Rev.*, 64(2), 020802.

AlQadi, I., AlHazmy, M., Al-Bahi, A., and Rodi, W. (2015). "Large eddy simulation of flow past tandem cylinders in a channel." *Flow Turbul. Combust.*, 95(4), 621–643.

ASCE. (1988). "Turbulence modeling of surface water flow and transport. Parts I–V." *J. Hydraul. Eng.*, 10.1061/(ASCE)0733-9429(1988)114:9(970), 970–1073.

Baggett, J. S., Jimenez, J., and Kravchenko, A. G. (1979). "Resolution requirements in large-eddy simulation of shear flows." *CTR Annual Research Briefs*, Stanford Univ., Stanford, CA.

Bedford, K. W., and Babajimopoulos, C. (1980). "Verifying lake transport models with spectral statistics." *J. Hydraul. Div.*, 106(1), 21–38.

Booij, R. (1989). "Depth-averaged k-ε modelling." *Proc., 23rd IAHR Congress*, IAHR, Delft, Netherlands.

Boussinesq, J. (1877). "Essai sur la théorie des eaux courantes." Mémoires présentés par divers savants à l'Académie des Sciences, Paris.

Bradshaw, P. (1971). *An introduction to turbulence and its measurement*, Pergamon Press, Oxford, U.K.

Burattini, P., Leonardi, S., Orlandi, P., and Antonia, R. A. (2008). "Comparison between experiments and direct numerical simulations in a channel flow with roughness on one wall." *J. Fluid Mech.*, 600, 403–426.

Burchard, H. (2002). *Applied turbulence modelling in marine waters, lecture notes in earth sciences 100*, Springer, Berlin.

Casey, M., and Wintergerste, T. (2000). *Best practice guidelines*, ERCOFTAC Publication.

Chan-Braun, C., Garcia-Villalba, M., and Uhlmann, M. (2011). "Force and torque acting on particles in a transitionally rough open-channel flow." *J. Fluid Mech.*, 684, 441–474.

Chan-Braun, C., Garcia-Villalba, M., and Uhlmann, M. (2013). "Spatial and temporal scales of force and torque acting on wall-mounted spherical particles in open channel-flow." *Phys. Fluids*, 25(7), 075103.

Chapman, D. R. (1979). "Computational aerodynamics development and outlook." *AIAA J.*, 17(12), 1293–1313.

Chaudhry, M. H. (2008). *Open-channel flow*, 2nd Ed., Springer, Berlin.

Chen, C. J., and Rodi, W. (1980). *Vertical turbulent buoyant jets: A review of experimental data*, Pergamon Press, Oxford, U.K.

Chow, V. T. (1959). *Open-channel hydraulics*, McGraw-Hill, New York.

Chua, S., McSherry, R., Stoesser, T., and Mulahasan, S. (2016). "Free surface flow over square bars at low and intermediate relative submergence." *J. Hydraul. Res.* (in press).

Davidson, P. A. (2004). *Turbulence: An introduction to scientists and engineers*, Oxford University Press, Oxford, U.K.

Davidson, P. A., Kaneda, Y., Moffatt, K., and Sreenivasan, K. R. (2011). *A voyage through turbulence*, Cambridge University Press, Cambridge, U.K.

Deardorff, J. (1970). "A numerical study of three-dimensional channel flow at large Reynolds numbers." *J. Fluid Mech.*, 41(2), 453–480.

Doneker, R. L., and Jirka, G. H. (1991). "Expert system for mixing-zone analysis and design of pollutant discharges." *J. Water Res. Plann. Manage.*, 10.1061/(ASCE)0733-9496(1991)117:6(679), 679–697.

Doneker, R. L., and Jirka, G. H. (2001). "CORMIX-GT system for mixing zone analysis of brine water disposal." *Desalination*, 139(1–3), 263–274.

Dong, S., Karniadakis, G. E., Ekmekci, A., and Rockwell, D. (2006). "A combined direct numerical simulation: Particle image velocimetry study of the turbulent near wake." *J. Fluid Mech.*, 569, 185–207.

Durbin, P., and Pettersson-Reif, B. A. (2001). *Statistical theory and modelling for turbulent flows*, Wiley, Hoboken, NJ.

Elder, J. W. (1959). "The dispersion of marked fluid in turbulent shear flow." *J. Fluid Mech.*, 5(4), 544–560.

Escauriaza, C., and Sotiropoulos, F. (2011). "Lagrangian model of bed-load transport in turbulent junction flows." *J. Fluid Mech.*, 666, 36–76.

Fang, H. W. (2000). "Three-dimensional calculations of flow and bed-load transport in the Elbe River." *Rep. No. 763*, Institut für Hydromechanik, Universität Karlsruhe, Karlsruhe, Germany.

Fischer, H. B., List, E. J., Koh, R. C. Y., Imberger, J., and Brooks, N. H. (1979). *Mixing in inland and coastal waters*, Academic, New York.

Fröhlich, J. (2006). *Large Eddy Simulation turbulenter Strömungen*, Teubner, Wiesbaden.

Galperin, B., and Orszag, S. A. (1993). *Large eddy simulation of complex engineering and geophysical flows*, Cambridge University Press, Cambridge, U.K.

Gauckler, P. (1868). "On the movement of water in pipes." *Ann. Ponts Chaussées*, 38(1), 229–281 (in French).

Grötzbach, G. (1979). "Numerical investigation of radial mixing capabilities in strongly buoyancy-influenced vertical turbulent channel flows." *Nucl. Eng. Des.*, 54(1), 49–66.

Hanjalic, K., and Launder, B. E. (2012). *Modelling turbulence in engineering and the environment*, Cambridge University Press, Cambridge, U.K.

Henderson, F. M. (1966). *Open channel flow*, Macmillan, London.

Herlina, H., and Wissink, J. G. (2014). "Direct numerical simulations of turbulent scalar transport across a flat surface." *J. Fluid Mech.*, 744, 217–249.

Hervouet, J. M., and Bates, P. (2000). "The Telemac modelling systems special issue." *Hydrol. Processes*, 14(13), 2207–2208.

Hinterberger, C., Froehlich, J., and Rodi, W. (2007). "Three-dimensional and depth-averaged large-eddy simulations of some shallow water flows." *J. Hydraul. Eng.*, 10.1061/(ASCE)0733-9429(2007)133:8(857), 857–872.

Hinterberger, C., Froehlich, J., and Rodi, W. (2008). "2D and 3D turbulent fluctuations in open-channel flow with $\mathrm{R}_\tau = 590$ studied by large eddy simulation." *Flow Turbul. Combust.*, 80(2), 225–253.

Hoyas, S., and Jimenez, J. (2006a). "Index of /~sergio." ⟨http://torroja.dmt.upm.es/~sergio⟩ (Apr. 2016).

Hoyas, S., and Jiménez, J. (2006b). "Scaling of the velocity fluctuations in turbulent channels up to $\mathrm{Re}_\tau = 2003$." *Phys. Fluids*, 18(1), 011702.

Ikeda, T., and Durbin, P. A. (2007). "Direct simulations of a rough-wall channel flow." *J. Fluid Mech.*, 571, 235–263.

Imberger, J., and Patterson, C. (1981). "A dynamic reservoir simulation model:DYRESM:5." *Transport models for inland and coastal waters*, H. B. Fischer, ed., Academic Press, Cambridge, MA.

Ishihara, T., Gotoh, T., and Kaneda, Y. (2009). "Study of high Reynolds number isotropic turbulence by direct numerical simulation." *Annu. Rev. Fluid Mech.*, 41, 165–180.

Kang, S., and Sotiropulos, F. (2012). "Assessing the predictive capabilities of isotropic, eddy viscosity Reynolds-averaged turbulence models in a natural-like meandering channel." *Water Resour. Res.*, 48(6), W06505.

Kempe, T., Vowinckel, B., and Froehlich, J. (2014). "On the relevance of collision modelling for interface-resolving simulations of sediment transport in open-channel flow." *Int. J. Multiphase Flow*, 58, 214–235.
Khosronejad, A., Kozarek, J. L., Palmsten, M. L., and Sotiropoulos, F. (2015). "Numerical simulation of large dunes in meandering streams and rivers with in-stream rock structures." *Adv. Water Resour.*, 81, 45–61.
Kidanemariam, A. (2015). "The formation of patterns in subaqueous sediment." Ph.D. thesis, Karlsruhe Institute of Technology, Karlsruhe, Germany.
Kidanemariam, A. G., and Uhlmann, M. (2014). "Direct numerical simulation of pattern formation in subaqueous sediment." *J. Fluid Mech.*, 750, R2.
Kim, J., Moin, P., and Moser, R. D. (1987). "Turbulence statistics in fully developed channel flow at low Reynolds number." *J. Fluid Mech.*, 177, 133–166.
Kline, S. J., Cantwell, B. J., and Lilley, G. M. (1981). *Proc. 1980-81 AFOSR-HTTM-Stanford Conf. on Complex Turbulent Flows: Comparison of Computations and Experiment*, Thermosciences Div., Dept. of Mechanical Engineering, Stanford Univ., Stanford, CA.
Kline, S. J., Morkovin, M. V., Sovran, G., and Cockrell, D. D. (1969). *Proc. Computation of Turbulent Boundary Layers–1968 AFOSR-IFP-Stanford Conf.*, Thermosciences Div., Dept. of Mechanical Engineering, Stanford Univ., Stanford, CA.
Kolmogorov, A. N. (1942). "The equations of turbulent motion in an incompressible fluid." *Izvestia Acad. Sci. USSR Phys.*, 6(1–2), 56–58.
Kuipers, J., and Vreugdenhil, C. B. (1973). "Calculations of two-dimensional horizontal flow." *Rep. S 163*, Delft Hydraulics Laboratory, Delft, Netherlands.
Lakehal, D., Krebs, P., Krijgsman, J., and Rodi, W. (1999). "Computing shear flow and sludge blanket in secondary clarifiers." *J. Hydraul. Eng.*, 10.1061/(ASCE)0733-9429(1999)125:3(253), 253–262.
Launder, B. E., and Rodi, W. (1983). "The turbulent wall jet: Measurements and modelling." *Annu. Rev. Fluid Mech.*, 15(1), 429–459.
Launder, B. E., and Sandham, N. D., eds. (2004). *Closure strategies for turbulent and transitional flows*, Cambridge University Press, Cambridge, U.K.
Launder, B. E. and Spalding, D. B. (1974). "The numerical computation of turbulent flow." *Comput. Methods. Appl. Mech. Eng.*, 3(2), 269–289.
Lea, L., Puertas, J., and Vazquez-Lenton, M. E. (2007). "Depth-average modelling of turbulent shallow water flow with wet-dry fronts." *Arch. Comput. Methods Eng.*, 14(3), 303–341.
Lee, M., and Moser, R. D. (2015). "Direct numerical simulation of turbulent channel flow up to $R_\tau = 5200$." *J. Fluid Mech.*, 774, 395–415.
Leendertse, J. J. (1967). "Aspects of a computational model for long-period water-wave propagation." Ph.D. dissertation, Rand Corporation, Santa Monica, CA.
Leonardi, S., Orlandi, P., and Antonia, R. A. (2007). "Properties of d- and k-type roughness in a turbulent channel flow." *Phys. Fluids*, 19(12), 125101.
Leschziner, M. (2016). *Statistical turbulence modelling for fluid mechanics: Demystified*, Imperial College Press, London.
Levi, E. (1995). *The science of water: The foundation of modern hydraulics*, ASCE, Reston, VA.
List, E. J. (1986). "Mechanics of turbulent buoyant jets and plumes." *Turbulent buoyant jets and plumes*, W. Rodi, ed., Pergamon Press, Oxford, U.K.
Lozano-Durán, A., and Jimenez, J. (2014). "Time-resolved evolution of coherent structures in turbulent channels: Characterization of eddies and cascades." *J. Fluid Mech.*, 759, 432–471.
Lyn, D. A. (2008). "Turbulence models for sediment transport engineering." *Sediment engineering*, M. H. Garcia, ed., ASCE, Reston, VA.
Manning, R. (1889). "On the flow of water in open channels and pipes." *Trans. Inst. Civ. Eng.*, 20, 161–207 (in Ireland).
Mellor, G. L., and Yamada, T. (1982). "Development of a turbulence closure model for geophysical fluid problems." *Rev. Geophys.*, 20(4), 851–875.
Menter, F. R. (1994). "Two-equation eddy viscosity turbulence models for engineering applications." *J. AIAA*, 32(8), 1598–1605.
Menter, F. R., and Egorov, Y. (2010). "The scale adaptive simulation method for unsteady flow predictions. Part I: Theory and model descriptions." *Flow Turbul. Combust.*, 85(1), 113–138.
Meyer-Peter, E., and Müller, R. (1948). "Formulas for bed-load transport." *Association of Hydraulic Research, 2nd Meeting*, IAHR, Delft, Netherlands.
Minh Duc, B. (1998). "Berechnung der Strömung und des Sedimenttransports in Flüssen mit einem tiefengemittelten numerischen Verfahren." Ph.D. thesis, Univ. of Karlsruhe, Karlsruhe, Germany (in German).
Moin, P., and Mahesh, K. (1998). "Direct numerical simulation: A tool in turbulence research." *Annu. Rev. Fluid Mech.*, 30(1), 539–578.
Moody, L. F. (1944). "Friction factors for pipe flow." *Trans. ASME*, 66(8), 671–684.
Nadaoka, K., and Yagi, H. (1998). "Shallow-water turbulence modeling and horizontal large-eddy computation of river flow." *J. Hydraul. Eng.*, 10.1061/(ASCE)0733-9429(1998)124:5(493), 493–500.
Naot, D., and Rodi, W. (1982). "Calculation of secondary currents in channel flow." *J. Hydraul. Div. ASCE*, 108(8), 948–968.
NASA. (1972). *Proc., Conf. on Free Turbulent Shear Flows*, NASA Langley Research Center, Hampton, VA.
Nezu, I., and Nakagawa, H. (1993). *Turbulence in open-channel flows, IAHR Monograph Series*, A.A. Balkema, Rotterdam, Netherlands.
Orszag, S. A., and Patterson, G. S. (1972). "Numerical simulation of three-dimensional homogeneous isotropic turbulence." *Phys. Rev. Lett.*, 28(2), 76–79.
Paik, J., Ge, L., and Sotiropoulos, F. (2004). "Toward the simulation of complex 3D shear flows using unsteady statistical turbulence models." *Int. J. Heat Fluid Flow*, 25(3), 513–527.
Palkin, E., Mullyadzhanov, R., Hadziabdic, M. and Hanjalic, K. (2016). "Scrutinizing URANS in shedding flows: The case of cylinder in cross flow in the subcritical regime." *Flow Turbul. Combust.*, 97(4), 1017–1046.
Pan, Y., and Banerjee, S. (1995). "A numerical study of free-surface turbulence in open channel flow." *Phys. Fluids*, 7(7), 1649–1664.
Patel, V. C., Rodi, W., and Scheuerer, G. (1985). "Turbulence models for near-wall and low Reynolds number flows." *AIAA J.*, 23(9), 1308–1319.
Piomelli, U. (2014). "Large eddy simulation in 2030 and beyond." *Philos. Trans. R. Soc. London, Ser. A*, 372(2022), 20130320.
Pope, S. B. (2000). *Turbulent flows*, Cambridge University Press, Cambridge, U.K.
Prandtl, L. (1925). "Über die ausgebildete Turbulenz." *Z. Angew. Math. Mech.*, 5, 136–139.
Prandtl, L. (1945). "Über ein neues Formelsystem für die ausgebildete Turbulenz." *Nach. Akad. Wiss. Göttingen, Math. Phys.*, K1, 6–19.
Rastogi, A. K., and Rodi, W. (1978). "Prediction of heat and mass transfer in open channels." *J. Hydraul. Div. ASCE*, 104(3), 397–420.
Reynolds, O. (1895). "On the dynamical theory of incompressible viscous fluids and the determination of the criterion." *Philos. Trans. R. Soc.*, 186, 123–164.
Reynolds, W. C. (1990). "The potential and limitations of direct and large eddy simulations." *Whither turbulence? Turbulence at the crossroads*, J. L. Lumley, ed., Springer, Berlin.
Rodi, W. (1980). *Turbulence models and their application in hydraulics: A state of the art review, IAHR monograph*, 1st Ed., A.A. Balkema, Rotterdam, Netherlands.
Rodi, W. (1984). "Examples of turbulence model applications, lecture IV: Two-dimensional depth-average calculations." *Turbulence models and their applications*, B. E. Launder, ed., Editions Eyrolles, Paris.
Rodi, W. (1987). "Examples of calculation methods for flow and mixing in stratified fluids." *J. Geophys. Res.*, 92(C5), 5305–5328.
Rodi, W. (1993a). "Elements of the theory of turbulence." *Coastal, estuarial and harbour engineers' reference book*, M. B. Abbott and W. A. Price, eds., Chapman and Hall, London.
Rodi, W. (1993b). *Turbulence models and their application in hydraulics: A state of the art review, IAHR monograph*, 3rd Ed., A.A. Balkema, Rotterdam, Netherlands.
Rodi, W. (1995). "Impact of Reynolds-average modelling in hydraulics." *Proc. R. Soc. London, Ser. A*, 415(1941), 141–164.

Rodi, W., Constantinescu, G., and Stoesser, T. (2013). *Large-eddy simulation in hydraulics, IAHR monograph*, CRC Press/A.A. Balkema, Boca Raton, FL.
Rodi, W., Pavlovic, R. N., and Srivatsa, S. K. (1981). "Prediction of flow and pollutant spreading in rivers." *Transport models for inland and coastal waters*, H. B. Fischer, ed., Academic Press, Cambridge, MA.
Rotta, J. C. (1951). "Statistische Theorie nichthomogener Turbulenz." *Z. f. Phys.*, 129(6), 547–572.
Rouse, H. (1946). *Elementary mechanics of fluids*, Wiley, Hoboken, NJ.
Santarelli, C., Roussel, J., and Fröhlich, J. (2016). "Budget analysis of the turbulent kinetic energy for bubbly flow in a vertical channel." *Chem. Eng. Sci.*, 141, 46–62.
Schmeeckle, M. W. (2014). "Numerical simulation of turbulence and sediment transport of medium sand." *J. Geophys. Res. Earth Sci.*, 119(6), 1240–1262.
Schumann, U. (1975). "Subgrid-scale model for finite-difference simulations of turbulent flows in plane channels and annuli." *J. Comput. Phys.*, 18(4), 376–404.
Smagorinsky, J. (1963). "General circulation experiments with the primitive equations. I: The basic experiment." *Mon. Weather Rev.*, 91(3), 99–164.
Sotiropoulos, F. (2015). "Hydraulics in the era of exponentially growing computer power." *J. Hydraul. Res.*, 53(5), 547–560.
Sotiropoulos, F., and Khosronejad, A. (2016). "Sand waves in environmental flows: Insights gained by coupling large-eddy simulation with morphodynamics." *Phys. Fluids*, 28(2), 021301.
Spalart, P. R., and Allmaras, S. R. (1994). "A one-equation turbulence model for aerodynamic flows." *La Recherche Aerospatiale*, 1, 5–21.
Spalart, P. R., Jou, W. H., Strelets, M., and Allmaras, S. R. (1997). "Comments on the feasibility of LES for wings, and on a hybrid RANS/LES approach." *Advances in LES/DNS, First AFOSR Int. Conf. on DNS/LES*, C. Liu and Z. Liu, eds., Greyden Press, Columbus, OH.
Stewart, R. W. (1969). "Turbulence, film." Education Development Center, Encyclopaedia Britannica Educational Corporation, Chicago.
Stoesser, T. (2014). "Large-eddy simulation in hydraulics: Quo vadis?" *J. Hydraul. Res.*, 52(4), 441–452.
Strickler, A. (1923). "Contributions to the question of velocity formula and the roughness numbers for rivers, channels and pipes." *Mitteilung 16*, C. Mutzner, ed., Amt für Wasserwirtschaft, Bern, Switzerland (in German).
Tennekes, H., and Lumley, J. L. (1972). *A first course in turbulence*, MIT Press, Cambridge, MA.
Thorenz, C. (2009). "Computational fluid dynamics in lock design: State of the art." *Int. Workshop*, PIANC, Brussels, Belgium.
Uijttewaal, W. S. J., and van Prooijnen, B. C. (2004). "Application of large-eddy simulation to shallow flows." *Proc. 6th. Int. Conf. on Hydroscience and Engineering*, Brisbane, Australia.
Uittenbogaard, R. E., and van Vossen, B. (2004). "Subgrid-scale model for quasi-2D turbulence in shallow water." *Shallow flows*, G. H. Jirka and W. S. J. Uijttewaal, eds., Taylor & Francis Group, London.
Van Rijn, L. (1993). *Principles of sediment transport in rivers, estuaries and coastal seas*, Aqua Publications, Blokzijl, Netherlands.
Venditti, J. G., and Church, M. A. (2005). "Bed form initiation from a flat sand bed." *Geophys. Res.*, 110(F1), F01009.
Violeau, D., and Rogers, B. D. (2016). "Smoothed particle hydrodynamics (SPH) for free-surface flows: Past, present and future." *J. Hydraul. Res.*, 54(1), 1–26.
Vowinkel, B., Kempe, T., and Fröhlich, J. (2014). "Fluid-particle interaction in turbulent open channel flow with full-resolved mobile beds." *Adv. Water Resour.*, 72, 32–44.
Vowinkel, B., Ramandeep, J., Kempe, T., and Fröhlich, J. (2016). "Entrainment of single particles in a turbulent open-channel flow: A numerical study." *J. Hydraul. Res.*, 54(2), 158–171.
Wallin, S., and Johansson, A. V. (2000). "An explicit algebraic Reynolds stress model for incompressible and compressible turbulent flows." *J. Fluid Mech.*, 403, 89–132.
Wenka, T., Brudy-Zippelius, T., and Schmidt, A. (2016). "2D and 3D modelling in German inland waterways." *Advances in hydroinformatics*, P. Goursbesville, et al., eds., Springer, Singapore.
Wilcox, D. C. (1993). *Turbulence modeling for CFD*, 1st Ed., DCW Industries, La Canada, CA.
Wilcox, D. C. (2006). *Turbulence modeling for CFD*, 3rd Ed., DCW Industries, La Canada, CA.
Wissink, J. G., and Rodi, W. (2008). "Numerical study of the near wake of a circular cylinder." *Int. J. Heat Fluid Flow*, 29(4), 1060–1070.
Wu, W. M., Rodi, W., and Wenka, T. (2000). "3D numerical modeling of flow and sediment transport in open channels." *J. Hydraul. Eng.*, 10.1061/(ASCE)0733-9429(2000)126:1(4), 4–15.
Wu, W. M., Wang, P., and Chiba, N. (2004). "Comparison of 5 depth-average 2D turbulence models for river flows." *Arch. Hydro. Eng. Environ. Mech.*, 51(2), 183–200.
Wu, X., and Moin, P. (2009). "Forest of hairpins in a low-Reynolds number zero-pressure-gradient flat-plate boundary layer." *Phys. Fluids*, 21(9), 091106.
Yakot, V., and Orszag, S. A. (1986). "Renormalization-group analysis of turbulence." *Phys. Rev. Lett.*, 57(14), 1722–1724.
Yamamoto, Y., Kunugi, T., and Serizawa, A. (2001). "Turbulence statistics and scalar transport in open-channel flow." *J. Turbul.*, 2(10), 1–16.